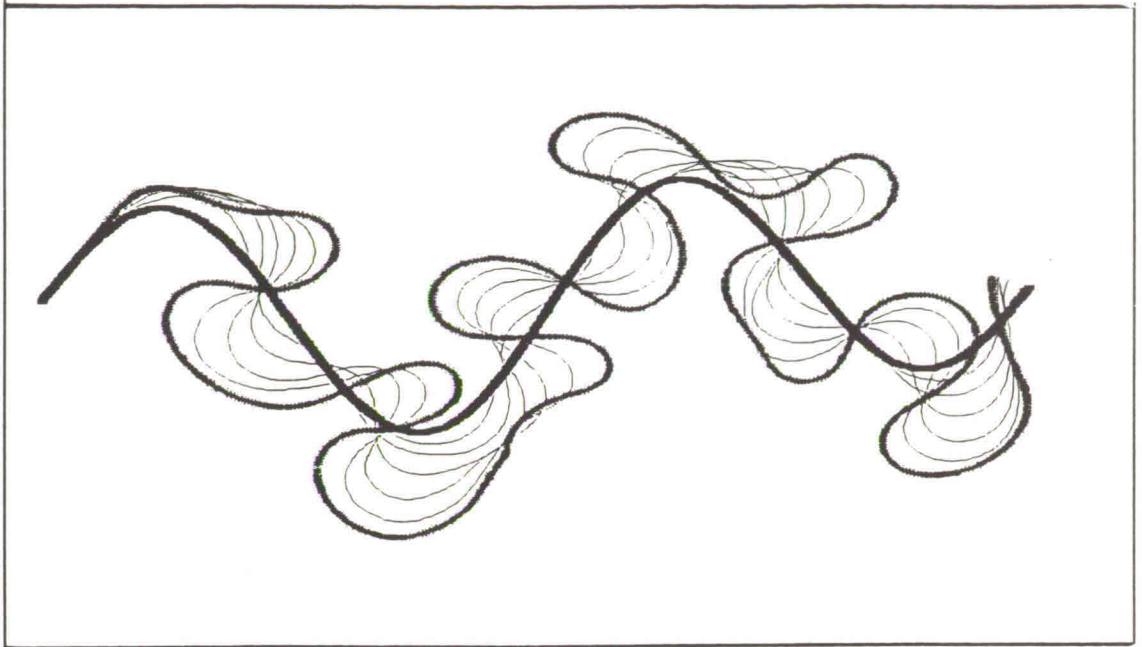


**International Institute for Infrastructural,
Hydraulic and Environmental Engineering**

Delft, The Netherlands.



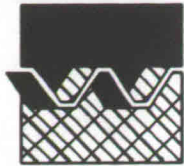
Maximum amplitude of river meanders

**Teresa de Jesús Soriano Pérez
Master of Science Thesis HH 206**

June, 1994.



**International Institute for Infrastructural,
Hydraulic and Environmental Engineering**



delft hydraulics

Maximum amplitude of river meanders

by Teresa de Jesús Soriano Pérez

**Master of Science Thesis
HH 206
Hydraulic Engineering**

**Examination Committee
Prof. B. Petry (IHE)
Ir. G.J. Klaassen (IHE, DH)
Dr. E. Mosselman (DH)**

June 23, 1994. Delft, The Netherlands

ABSTRACT

The prediction of planform changes is important for the site selection of structure like bridges or intakes. In the design of bank protection works it is indispensable to know future planform developments for the safety of structures and lands.

The meander development process consists of translation and expansion of the bends due to bank erosion. A characteristic feature of curved flow is the spiral flow. The effect of flow through a river bend is erosion along the outer banks, while deposition of material along the inner banks takes place. The curvature of meander bends changes continuously during the bank erosion implying a variation of the lateral bed slope and a continuous process of redistribution of the flow and sediment transport.

Mathematical models are becoming increasingly important. They are used for the prediction of planform development of meandering rivers. The 2-D MIANDRAS model of Crosato (1990) used in this study, through via this improved bank erosion model considers, in determining of the erosion rate, to be proportional to the excess near-banks flow velocities to a critical value. Different from the earlier version of the model, the critical flow velocity was assumed to be constant and therefore different from the zero-order flow velocity.

The existing bank erosion models consider an immediate reduction of the longitudinal bed slope, being true for the cases with fast bank erosion. In this study the real longitudinal bed slope is determined, accounting for the different time-scales of the two processes involved, notably the bank erosion (lateral growth of river bends due to the fact that sinuosity increases) and the longitudinal aggradation of the bed. The results are based on numerical simulations from the 1-D WENDY model developed by DELFT HYDRAULICS.

The reduction in flow velocity due to the increasing sinuosity was studied as cause of reaching a maximum amplitude of meander bends. For this purpose numerical simulations were carried out with the MIANDRAS program developed by Crosato (1990). The model proposed was adapted the bank erosion module of the MIANDRAS program. In this study was found that many parameters influence the development of bends, notably geometry, discharge, channel width, the interaction parameter (λ_s/λ_w), the wave length (L_p) and the damping length (L_D) of the bed deformation. The translation of bends is dominant for high values of L_p , being an important result for determining the maximum amplitude of river bends.

ACKNOWLEDGEMENTS

This thesis is the result of a study performed at DELFT HYDRAULICS, location '*de Voorst*', The Netherlands.

I wish to express my gratitude to Instituto Mexicano de Tecnología del Agua and Comisión Nacional del Agua, my sponsor, and I hope they continue their labour of supporting mexican engineers.

My acknowledgement to Ir G.J. Klaassen and Dr. E. Mosselman for their guidance, support and contribution, from them I learn always something during our discussions. Thanks to Mr. C. Flokstra for his contribution.

I would like to express my thanks to Prof. B. Petry, for his support and comments to this study. Thanks to Ir. R. de Heer for his comprehension and support.

Special thanks to all my close friends for their support. Thanks to my parents and all my family back in Mexico.

This thesis is dedicated to the memory of Dr. Enzo Levi

Teresa de Jesús Soriano Pérez
Delft, June 23 1994.

CONTENTS

ABSTRACT	i
ACKNOWLEDGEMENTS	ii
CONTENTS	iii
LIST OF FIGURES AND TABLES	v
LIST OF SYMBOLS	vii
1. GENERAL	
1.1 Introduction	1.1
1.2 Water motion in meandering rivers	1.4
1.3 Geometry of meanders	1.5
1.4 Causes of maximum amplitude of river bends.....	1.6
1.4.1 Geological confinement	1.6
1.4.2 Bend cutoffs	1.7
1.4.3 Flow velocity reduction due to sinuosity increase	1.7
1.4.4 Nonlinear effects	1.7
1.5 Aim of the study	1.8
1.6 Approach	1.8
2. PREVIOUS WORK	
2.1 Classification of meandering rivers	2.1
2.2 Empirical relations	2.4
2.3 Mathematical models	2.6
2.3.1 Flow and bed topography models	2.6
2.3.2 Bank erosion models	2.7
3. REVIEW OF MIANDRAS MODEL	
3.1 General	3.1
3.2 Behaviour of the MIANDRAS model	3.3
3.3 Modifications to the MIANDRAS model	3.6

4. INVESTIGATIONS

4.1 General	4.1
4.2 Slope reduction	4.2
4.2.1 Approach	4.2
4.2.2 Time-scales	4.4
4.2.3 Results	4.7
4.2.4 Importance of the bed slope reduction	4.13
4.2.5 Conclusions	4.15
4.3 Effect of considering $u_c = u_o$ in the bank erosion model	4.16
4.4 Proposed bank erosion model $u_c \neq u_o$	4.18
4.5 Numerical simulations	4.18
4.5.1 Sensitivity analysis of parameters	4.19
4.5.2 Critical flow velocities and maximum amplitude of river bends	4.25

5. CONCLUSIONS AND RECOMMENDATIONS**APPENDIX A****REFERENCES**

LIST OF FIGURES AND TABLES

FIGURES

- 1.1.1.- Planforms of Fluvial Systems (Simons, 1983)
- 1.1.2.- Meander migration
- 1.1.3.- Bank erosion and meander development of different rivers
- 1.2.1.- Physical process in meandering rivers
- 1.3.1.- Definition sketch for meanders
- 1.4.1.1.- Confined meandering
- 1.4.2.1.- Bend cutoff

- 2.1.1.- Classification of meanders according to Brice (1983)
- 2.1.2.- Classification of meanders according to Ikeda (1989)

- 3.1.1.- Longitudinal and transversal profile of the bed, Crosato (1990)
- 3.1.2.- Bank erosion model of MIANDRAS
- 3.2.1.- Longitudinal profile of the bed along the outer bend
- 3.2.2.- Relative wave number and damping coefficient as a function of λ_s/λ_w .
- 3.2.3.- Variation of damping coefficient and wave number due to changes of the exponent b
- 3.3.1.- Proposed bank erosion model

- 4.1.1.- Bank erosion process
- 4.2.1.1.- Schematization of the reduction of the bed slope
- 4.2.1.2.- Configuration used in the numerical simulations
- 4.2.2.1.- Slope reduction due to the increase of sinuosity
- 4.2.2.2.- Adaptation of the bed slope due to aggradation
- 4.2.3.1.- Adaptation of the longitudinal bed slope for $L = 10$ km
- 4.2.3.2.- Adaptation of the longitudinal bed slope for $L = 5$ km
- 4.2.3.3.- Adaptation of the longitudinal bed slope for $L = 10$ km
- 4.2.3.4.- Adaptation of the longitudinal bed slope for $L = 20$ km
- 4.2.3.5.- Adaptation of the longitudinal bed slope for $L = 25$ km
- 4.2.3.6.- Time-scales ratio
- 4.2.3.7.- Time-scales ratio
- 4.2.4.1.- Time-scales ratio for different rivers
- 4.3.1.- Model results considering $u_c = u_o$
- 4.3.2.- Model results considering $u_c < > u_o$
- 4.5.1.1.- Planimetry of the hypothetical river
- 4.5.1.2.- Planform development of bends with constant discharge
- 4.5.1.3.- Planform development of bends with variable discharge
- 4.5.1.4.- Planform development of bends with different widths
- 4.5.1.5.- Planform development of bends with different roughness
- 4.5.1.6.- Planform development of bends with different bed material
- 4.5.1.7.- Influence of the exponent b (sediment transport formula)
- 4.5.2.1.- Planform development
- 4.5.2.2.- Flow profile at both banks
- 4.5.2.3.- Planform development
- 4.5.2.4.- Planform development
- 4.5.2.5.- Planform development with finite amplitude

- A.1.- The curvilinear co-ordinate system

TABLES

- 2.1.1.- Empirical relationships between wave length (λ) and width (w)
- 2.1.2.- Empirical relationships between amplitude (a) and width (w)
- 2.1.3.- Empirical relationships between wave length (λ) and bankfull discharge (Q)

- 4.2.4.1.- Characteristics of some rivers in the world
- 4.5.1.1.- Parameters used in the numerical simulations

LIST OF SYMBOLS

a	amplitude of bends
A	coefficient
α	coefficient
b	exponent of the transport formula
c_b	celerity of the bed disturbance
C	Chézy coefficient
C_E	bank erosion rate according to Hickin & Nanson (1984)
Δ	relative submerged density of the sediment
Δx	space-step
Δt	time-step
D_{50}	median particle size of bed material
E	parameter
E_h	bank-instability-induced bank erosion coefficient
E_u	flow-induced bank erosion coefficient
$f(\theta)$	weighing function
Fr	Froude number
g	acceleration due to gravity
σ	coefficient
h	water depth
H'	total deformation of water depth
h'	water depth deformation due to redistribution of flow and sediment
i	bed slope
i_s	equilibrium bed slope
i_v	valley slope
κ	Von Karman constant
L	length
λ	wave length of the bend
λ_s	adaptation length of the bed
λ_w	adaptation length of the flow
L_D	damping length of the bed disturbance
L_p	wave length of the bed disturbance
m	mode that determines the transversal pattern
p	sinuosity
Q	discharge
r	radius of curvature
r_1	interaction parameter
ρ	fluid density
$R \times$	effective local radius of curvature of the stream-line
s	sediment transport per unit of width

S	total volumetric sediment transport
s_n	volumetric component of the sediment transport in n direction per unit of width
s_s	volumetric component of the sediment transport in s direction per unit of width
θ	Shields parameter
t	time
τ_B	shear stress
τ_c	critical shear stress
T_e	time-scale of the bank erosion (sinuosity increases)
T_{long}	time-scale of the longitudinal aggradation
u	depth-averaged tangential velocity
u_o	average flow velocity
U'	total deformation of flow velocity
u'	flow velocity deformation due to redistribution of flow and sediment
v	depth-averaged transverse velocity
w	width
ζ	constant
Y_b	opposing force per unit boundary area
z_b	bed level
z_w	water level

1. GENERAL

1.1 Introduction

Alluvial rivers are usually classified in three categories according to their channel patterns (see figure 1.1.1): straight, meandering and braided (Leopold and Wolman, 1957). A meandering river consists of a number of consecutive bends. The present study is focused only on meandering rivers.

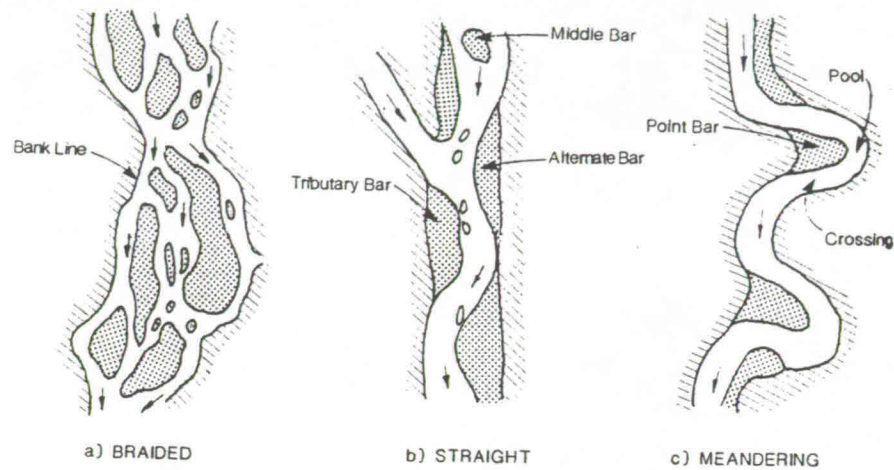


Figure 1.1.1 Planforms of Fluvial Systems (Simons, 1983)

The fluvial processes encountered in natural meandering rivers have been studied by many researchers for centuries. Not only does the geometric shape of river bends give rise to a complicated three-dimensional flow field, but equally importantly, the flow field reshapes the bends through the process of bank erosion.

The meander development consists of translation and expansion of their bends due to bank erosion, see figure 1.1.2.

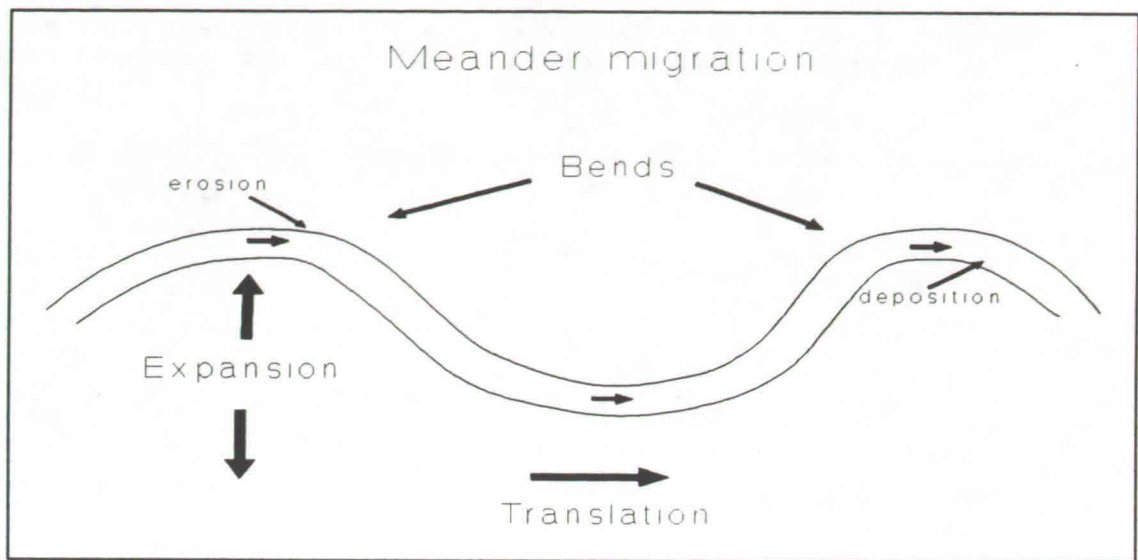


Figure 1.1-2.

A characteristic feature of curved flows is the spiral (helical) flow, outward near the surface and inward near the bottom; along the outer bend the movement is downward and along the inner bend the motion is directed upward. The effect of flow through a river bend with erodible banks is erosion along the outer banks and together with deposition of material along the inner banks.

Flow parameters may be the most important factors in the bank erosion process. The shear stress on the banks or near-bank flow velocity is the most important parameter. The magnitude of the discharge will determine the velocity and water depth within the rivers which directly affect the bank stability. The channel slope is also an important factor, this controls the flow velocity: as slope decreases, the flow velocity and the shear stress decreases, the river bank stability will increase. Other factors having influence on the bank erosion process are the biological factors and man induced factors. Some examples of meander development of different rivers are given in figure 1.1.3.

Bank material characteristics play an important role in the bank erosion process. The bank material eroded participates in the sediment transport process. River banks can be categorized into four general types of material: cohesive, non-cohesive, stratified and rock.

The prediction of planform changes of rivers is important for several reasons. For example, for site selection of a bridge or an intake structure, it is invaluable to know the present and future attack of the river on those structures. Secondly, when protecting existing structures from a migrating river, by bank protection or other methods, it is necessary to quantify the response of the rivers to different engineering solutions. Thirdly, a migrating river may be

eroding valuable property and having some tools for estimating the rate at which this is happening, is of considerable interest in the assessment of the economic feasibility of protection works. Initially it is important to be able to estimate the total width occupied by a meandering river, e.g. when planning the alignment of adjacent levees. This holds even more in cases where the regime of the river is affected by upstream developments (reservoirs, diversions) which may change the regime of the meandering river substantially. Therefore, it is important to be able to predict the maximum amplitude of meander, which implies that lateral bank erosion stops and no more damages will be produced outside the width of meandering trends.

Meandering rivers can reach a maximum amplitude (finite) due to: *reduction of the flow velocity* because of sinuosity increases during meander development, *cutoffs*: intersection of two river loops, *topographic confinement*: the existence of resistant material (rock) or the high banks (hills, bluffs), and *nonlinear effects*: geometrical nonlinearities produce skewing and fattening of meanders bends, Parker et al. (1982).

There are many theories that attempt to explain the causes of initiation and development of meanders, because of the complex behaviour of meandering rivers. But even now, the physical process is not well understood. The present study does not address the initiation of meandering, but rather concentrates on the fate of already existing meanders.

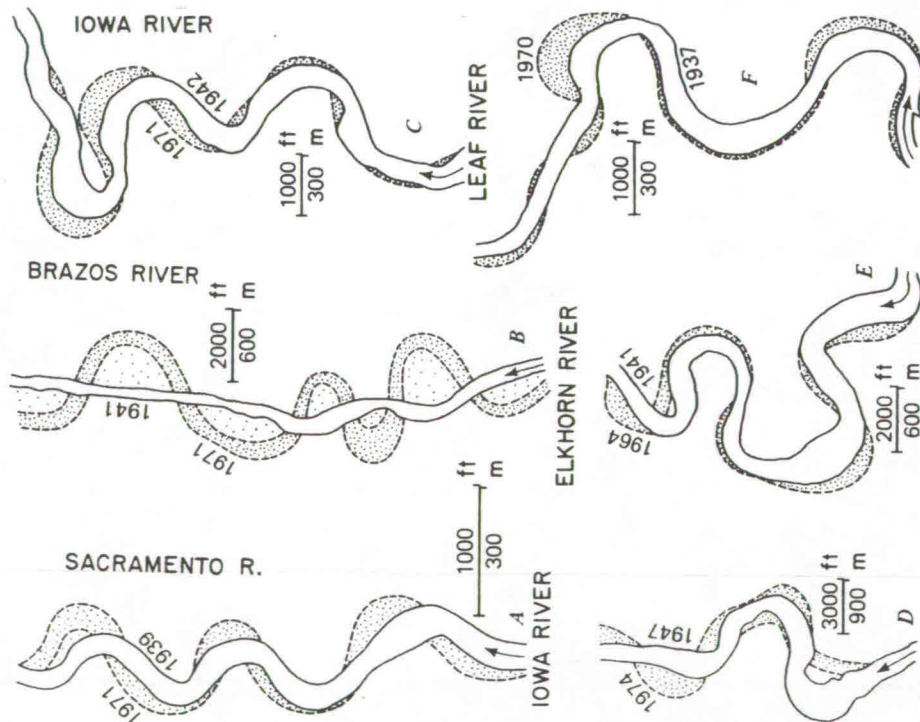


Figure 1.1.3. Bank erosion and meander development of different rivers

1.2 Water motion in meandering rivers

During the migration the river bends change their curvature and bed topography resulting in a complicated flow distribution. Around the entrance of the bend the transverse water surface slope will grow rapidly from zero until its final value in the bend. So, along the inner bank the longitudinal water surface slope will increase rapidly and cause an acceleration of the flow there. Along the outer bank the slope decreases and the flow decelerates. In turn this ensures a gradual growth of the streamline curvature around the entrance. The secondary flow will also grow gradually as it will establish a transverse bed slope.

The centripetal acceleration of the water particles in a river bend is established by a transverse slope of the water surface, implying that the centripetal acceleration is uniformly distributed over the vertical (hydrostatic pressure distribution). As the longitudinal flow velocity increases from zero at the bed until its maximum at or close to the water surface the flow close to the bottom will follow a path with a smaller radius of curvature than the flow closer to the water surface, i.e. the flow will form a spiral motion. See figure 1.2.1.

The secondary flow is directed towards the centre of curvature near the bottom and outwards in the upper part of the cross-section. In the central part of the flow horizontal convection is dominant, whereas vertical convection is dominant close to the banks. The net influence of secondary flow convection is an increase of the main flow velocity in the outer bend and reduction in the inner part. The main flow will adapt to the changing bed topography (bed friction) and to the influence of secondary flow convection, i.e. the main flow velocity will increase in the outer bend, the first effect being by far the most important.

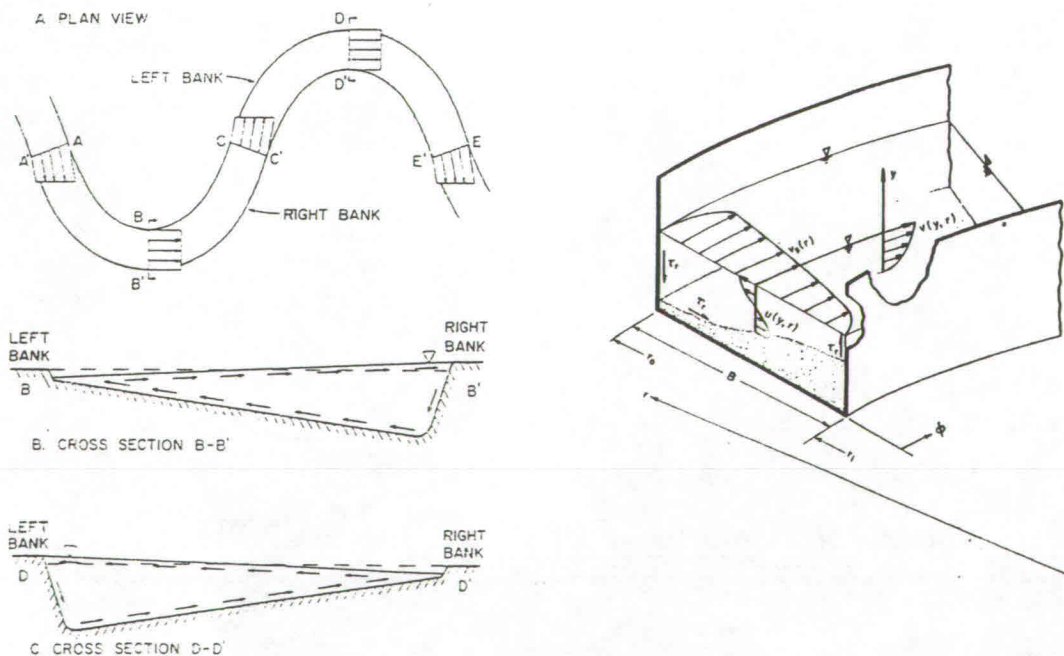


Figure 1.2.1 Physical process in meandering rivers

1.3 Geometry of meanders

The characteristics that define the plan geometry of meandering channels are showed in the figure. 1.3.1, which gives an idealized picture of a meander. In reality meanders are much more irregular (see also figure 1.1.3), which makes the determination of meanders characteristics more difficult. Often the meander train is split at the inflection points, and the characteristics of the individual meanders are averaged.

- l meander length
- λ wave length
- a amplitude
- r radius of curvature
- w width

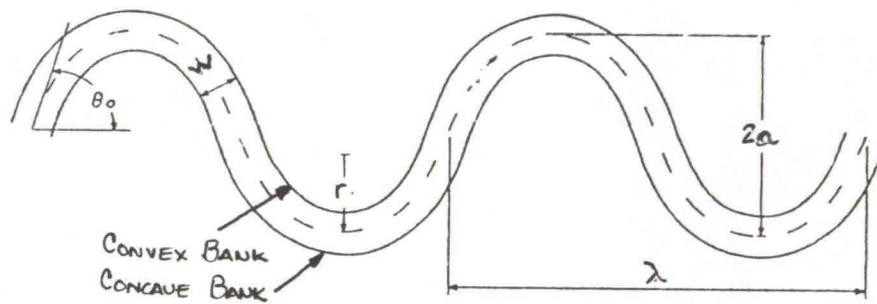


Figure 1.3.1.- Definition sketch for meanders

The sinuosity is the ratio between the meander length and the wave length:

$$P = \frac{l}{\lambda}$$

also it can be in equilibrium conditions also computed as the ratio of the valley slope and the river slope:

$$P = \frac{i_v}{i}$$

The sinuosity of river channels is clearly apparent in maps and aerial photographs, where the successive curves of a river often appear to have a certain regularity.

1.4. Causes of maximum amplitude of river bends

Many factors influence bank erosion processes in the river. Among these are: hydraulic parameters (fluid properties, flow characteristics), characteristics of bed and bank material (size, gradation, shape, etc.), geometry and structure of banks (height, slope, cohesive, cohesion, stratification, rock), biological factors (vegetation such as grass, shrubs, and trees), and man induced factors (agriculture, urbanization, drainage, floodplain development, bank protection, etc.).

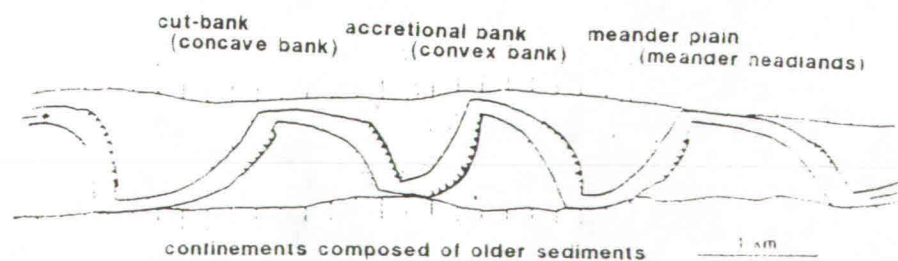
River bends can not grow to infinity and reach a maximum amplitude. Some of the possible causes of reaching a maximum amplitude are: geological confinement, bend cutoffs, reduction of flow velocities due to sinuosity increase, and nonlinear effects.

1.4.1 Geological confinement

The characteristics of the soil play an important role in the planform development of meanders. The shape and size of the bends are strongly influenced by the geological composition of banks and flood plains.

For instance, the meanders will have a finite amplitude when the flood plains consist of rock, the river banks can not be erode, so there is only translation of the river bends. For this case the geological characteristics of the floods plains act as boundary restriction. A typical example is shown in Figure 1.4.1.1. Also the meanders reach a maximum amplitude because of the existence of high bank (hills, bluffs).

In Chapter 2 a classification of meandering rivers on the basis of geological confinement according to Ikeda (1989) is presented.



A meandering channel is compelled to bend abruptly when the channel impinges on confinements in a restricted or confined meandering channel. [Based on map of Sundborg, 1956].

Figure 1.4.1.1- Confined meandering

1.4.2 Bend cutoffs

On natural streams, individual loops are diverse in form. The shape of river bends change continuously when they migrate. Cutoffs are defined as a process by which an alluvial river flowing along curves or bends abandons a particular bend and establishes its main flow along a comparatively straighter and shorter channel (Joglekar, 1971). Since the river abandons its old channel a finite amplitude is reached (instantaneous), the new channel of the river will start to develop, see figure 1.4.2.1.

Whether or not a cutoff will be developed during the high stage of flood depends on many parameters as: cutoff ratio, roughness, vegetation and erodability of the flood plain, magnitude and duration of the flood wave, the geometry of the bifurcation, etc. See for more details Klaassen & van Zantein (1989) and Klaassen (1992).

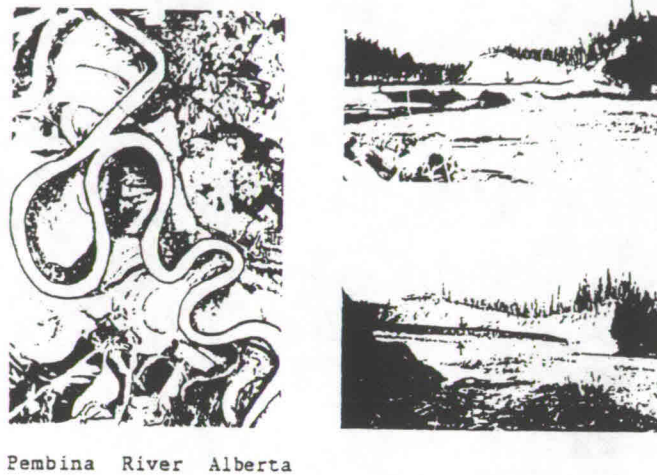


Figure 1.4.2.1.- Bend cutoff.

1.4.3 Flow velocity reduction due to sinuosity increase

During the planform development the river bends grow laterally producing an increase of river length and sinuosity. Assuming the overall water level difference between upstream and downstream to remain the same the river bed slope and the flow velocity decrease. The bank erosion rate decreases until the near-bank flow velocities are lower than the critical velocity for eroding banks.

1.4.4 Nonlinear effects

According to Parker et al. (1982) meander bends can reach a maximum amplitude because the geometrical nonlinearities, producing skewing and fattening of meander bends.

1.5 Aim of the study

The present study aims at the investigation of river bends with finite amplitude. The reduction in flow velocity due to the increasing sinuosity is considered as cause of reaching maximum amplitude of bends. The understanding of the mechanism of the bank erosion process in meandering rivers is a fundamental part of this study.

1.6 Approach

This study is based only on numerical simulations with the quasi 2-D mathematical model MIANDRAS, through via the proposed improved bank erosion model. Different from the earlier model version is that the critical flow velocity for eroding banks takes into account the property of the soils. The bank erosion is computed at both banks. Hypothetical planimetries are used.

Through the determination of the most important parameters in the development of bends the maximum amplitude is achieved. Once it is known the influence of the parameters it can be determined when lateral grow of bends is dominant during the migration process.

The MIANDRAS model does not consider the time-scale of the bank erosion process when sinuosity increases and the time-scale of the longitudinal aggradation of the bed. In the determination of the longitudinal bed slope has to be considered the time-scales of both processes. The longitudinal bed slope is computed through numerical simulations using the 1-D WENDY model. The increase in sinuosity and the longitudinal aggradation of the bed are reproduced simultaneously with the scheme adopted.

2. PREVIOUS WORK

2.1 Classification of meandering rivers

Meandering rivers can be classified on the basis of: *planform properties* and *geological confinement*.

Planform properties

According to Brice (1983) three types of meandering rivers can be distinguished. Planform properties of meandering rivers include not only the geometry and sinuosity of the meandering course, but other properties such as variability of width and development of bars. See figure 2.1.1.

Sinuuous canaliform.- it is characterized by narrow crescent-shaped point bars, a notably uniform width, a lack of braiding, and a moderate to high sinuosity. This river type tends to be associated with a substantial degree of bank resistance (owing either to bank vegetation or to clay content) relative to slope and discharge. The bed material is typically sand or silt, but it may be gravel.

Sinuuous point bar.- rivers tend to increase in width at the apexes of bends, and to have prominent bare point bars that are visible at normal stage. Point bars are typically scrolled, although the prominence of these scrolls is highly variable from one river to another. Bank resistance is lower, relative to slope and discharge, than for canaliform rivers. Bed material is commonly sand or gravel, but with an increasing proportion of gravel the bends tend to become more irregular, especially on smaller rivers.

Sinuuous braided.- with a further decrease in bank resistance, or quantity of bed-material load increases, the degree of braiding increases, point bars become more irregular and braided, and the river type changes to sinuous braided.

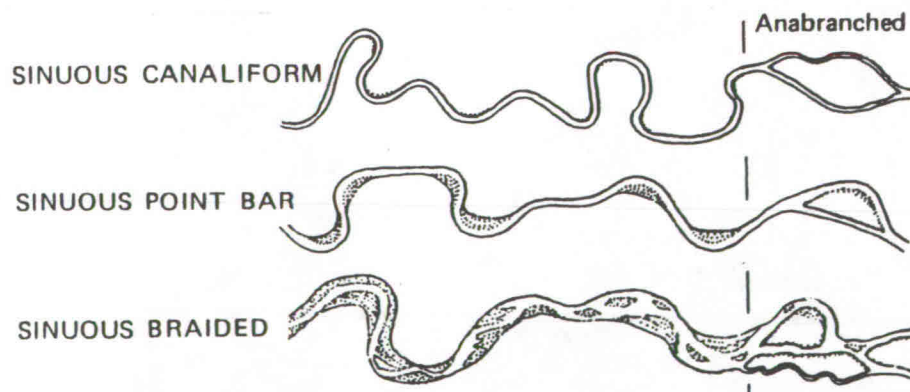


Figure 2.1.1. Classification of meanders according to Brice (1983).

Geological confinement

Ikeda (1989) makes a classification of meandering channels into four types: a) fixed meanders, b) restricted meanders, c) confined free meanders and d) truly free meanders, see figure 2.1.2.

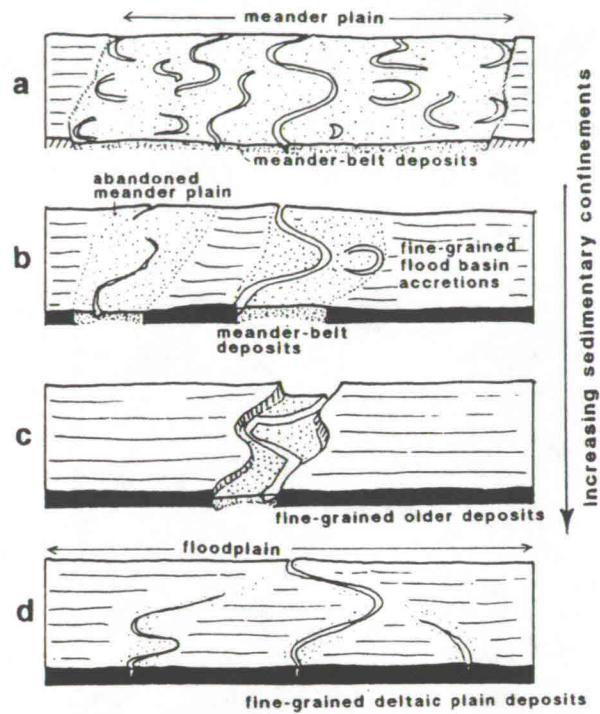
Truly free meanders (without fine-grained flood basin accumulations).- As its name indicates, a meandering river migrates freely over the entire flood plains without confinements within it.

Confined free meanders (developed on aggraded flood plains).- On a sufficiently large flood plain or a relatively slowly migrating meander belt, thick accumulations of fine sediment mixed with organic matter produced in a swampy environment will develop adjacent to the meander belt; there serve to confine it to a region wider than individual bends but much narrower than the entire flood plain.

Restricted meanders (formed by incised channels onto Deltaic Plains).-The sinuosity of restricted meandering channel changes in time. The migration rate of the channel, and therefore, the rates of reworking and accumulation of sediment are also influenced by the planform on the confined trough. The channel impinges the confined wall and hugs the wall for mo distance until a bend is initiated toward the opposite trough wall. It seems that concave-bank benches are well developed in restricted meandering rivers.

Fixed meanders (in Deltaic plains).- A channel in a deltaic plan has rather straight reaches. But, at the river mouth if a delta stream, a mid-channel shoal tends to develop. These often become bars and eventually islands which bifurcate the channels. The entrenchment of the channel bed occur due to the lowest part of the deltaic channel bed rises toward a seaward bar, so that as channel advances it must incise through the mouth bar and delta-front deposits. These deposits are cohesive and retard channel migration, leading to a "fixed" channel.

It is important the classification made by Ikeda (1989), since river bends can reach a maximum amplitude due to the presence of resistant material.



Types of alluvial meanders classified by degree of sedimentary controls on channel shifts. (a) truly free meanders, arisen from a deficiency of fine-grained sediment supply, (b) confined free meanders formed by a high supply of fine-grained sediment, (c) restricted meanders with confinement consisting of older cohesive deposits, (d) fixed meanders on deltaic plains.

Figure 2.1.2

2.2 Empirical relations

Several researchers have reported the empirical relations of meander parameters for rivers in alluvial materials. Some empirical equations are quite similar, meanwhile others are completely different. This is because they are based on rivers with different characteristics. In general these equations can be expressed as:

$$\lambda = c_1 w^{c_2}$$

$$\lambda = c_3 Q^{c_4}$$

$$a = k_1 w^{k_2}$$

where

Q	discharge	[m ³ /s]
c ₁ , c ₂ , c ₃ , c ₄ , k ₁ , k ₂	constants	[-]

The next tables show some of the equations that relate the different meander parameters, established by several researchers.

Equation	Source
$\lambda = 6.60 w^{0.99}$	Inglis, 1949 (Ferguson data)
$\lambda = 10.90 w^{1.01}$	Leopold & Wolman 1960
$\lambda = 10.00 w^{1.025}$	Zeller, 1967
$\lambda = 12.13 w^{1.09}$	Ackers & Charlton, 1970
$\lambda = 17.20 w$	Gorycki, 1960

Table 2.1.1 Empirical relationships between wave length (λ) and width (w), SI units.

Equation	Source
$a = 18.6 w^{0.99}$	Inglis, 1949 (Ferguson data)
$a = 10.9 w^{1.04}$	Inglis, 1949 (Bates data)
$a = 2.7 w^{1.1}$	Leopold & Wolman, 1957
$a = 4.5 w$	Zeller, 1967
$a = 14.0 w$	Bates, 1944
$a = 18-20 w$	Dury, 1954
$a = 12.15 w$	Altunin, 1949

Table 2.1.2 Empirical relationships between amplitude (a) and width (w), SI units.

The exponents in the regression equations are in many cases close to unity. This means that relations between wave length (λ), amplitude (a), and channel width (w) may be considered linear.

Equation	Source
$\lambda = 54.0 Q^{0.5}$	Inglis, 1949
$\lambda = 32.9 Q^{0.55}$	Leopold & Wolman, 1957
$\lambda = 54.3 Q^{0.5}$	Dury, 1965
$\lambda = 11.55 Q^{0.75}$	Agarwal, 1941
$\lambda = 61.2 Q^{0.47}$	Blench, 1910

Table 2.1.3 Empirical relationships between wave length (λ) and bankfull discharge (Q), SI units.

Other relationships:

$$\lambda = 4.7 r^{0.98}$$

Leopold & Wolman, 1957, SI units.

$$\lambda = 3.5 (w/h)^{-0.27}$$

Schumm, 1968 (h = water depth), SI units.

$$r = (\lambda/13) p^{1.5}/(p-1)^{0.5} \quad \text{Langbein, 1966.}$$

$$r = 3.1 w p^{-0.79} \quad \text{H.W. Shen, 1988.}$$

Leopold & Wolman state explicitly that correlation between a and w is poor.

According to these empirical relationships the amplitude is function of the channel width. The magnitude of the amplitude can be 3 to 20 times the channel width, this is wide range. It is difficult to know which relation it will be the most appropriate for the river under study. Therefore the geometry of meanders can be determined by using mathematical models.

2.3 MATHEMATICAL MODELS

Physical or mathematical models are often applied in order to assess morphological changes. Such models are well suited for prediction of morphological changes taking place on large time and length scales. Several attempts have been made to understand the basic mechanisms of meander formation. In a morphological model four aspects are important, the computation of the flow distribution, the sediment transport, the bed level variation and the bank erosion rate.

A summary of some mathematical models that compute the flow field, the bed topography and bank erosion processes is presented with some of the underlying assumptions.

2.3.1 FLOW FIELD AND BED TOPOGRAPHY MODELS

ENGELUND (1974) was the first investigator who considered the redistribution effects of the flow and sediment transport, he investigated the equilibrium flow and bed topography in a channel with sinusoidal curvature variation using a simple flow model that accounts for bed friction and main flow inertia. By means of a mainly linear solution procedure of the model he obtained good agreement between theoretical and experimental results. This model is the foundation on which all the remaining ones have been built.

IKEDA's et al. (1981) model is derived from ENGELUND's (1974) model. Their approach is that of a small perturbation in which the small parameter is the channel half-width over the minimum radius of curvature of the channel centreline. They assumed the transverse bed slope to be a function only of local channel centreline curvature.

STRIKSMAN et al. (1985) observes that a significant part of the lateral bed slope in bends can be due to an "overshoot" effect induced by the redistribution of water and sediment in the first part of the bend. Their model assumes a steady deformation of flow and channel bed is the alternate bar type caused by an upstream flow disturbance.

BLONDEAUX & SEMINARA (1985) base their model on fully coupling flow field, bed topography and sediment transport introducing in this way the flow-redistribution effect. Their model is linear which allows for an analytical solution for some simple channel geometries.

They indicate in their experimental and theoretical findings that the lateral bed slope at, or just downstream of, the entrance to a bend can be substantially higher than the slope obtained if the flow is assumed to be fully adapted to the bend curvature, as may be the case farther downstream.

The model of ODGAARD (1986 a,b) is based on essentially the same equations as the IKEDA et al. (1981). He assumes that the transverse bed slope is determined by the strength of the helical flow, and obtained an equation for the transverse bed slope that encompasses the overdeepening of Struiksma et al. (1985).

The model of BECK (1988) is essentially the same as IKEDA et al. (1981), except that the transverse bed slope is no longer a function only of local centreline curve. BECK (1988) assumes a semi-empirical relation, when calculating the bed topography, rather than attempting to satisfy sediment continuity.

2.3.2 BANK EROSION MODELS

HICKIN & NANSON (1975) suggest the existence of a relationship between the outward normal migration rate and the ratio of channel half-width, w , to channel centreline radius of curvature, r . HICKIN (1974) suggested, based on field observations, considers that the underlying physical process driving bank erosion is the shear stress, exerted on the bank by the primary flow. HICKIN & NANSON (1984) find that the bank erosion rate is a function of the curvature radius to width, r/w , with a maximum value at $r/w=2.5$. This result is based on the study of several sand rivers in Canada. According to them the rate of channel migration, M , depends on: bend radius, r ; channel width, w , bank height, h ; stream power, w_o , and the opposing force, Y_b . The next equations compute the bank erosion rate:

if $r/w > 2.5$

$$M = \frac{2.5 M_{2.5}}{\frac{r}{w}}$$

if $r/w < 2.5$

$$M = \frac{\frac{r}{w} - 1}{M_{2.5} 1.5}$$

and

$$M_{2.5} = \frac{w_o}{h Y_b}$$

ARIATHURI & ARULANANDAN (1978) develop a simple relation for the rate of erosion of cohesive soils. According to them the rate of bank retreat is directly proportional to the difference between the flow shear-stress on the bank, τ_B , and the critical shear stress one, τ_c , below which no erosion occurs:

$$\frac{\partial n}{\partial t} = \xi \frac{\tau_B - \tau_c}{\tau_c} \quad \text{for } \tau_B \geq \tau_c$$

$$\frac{\partial n}{\partial t} = 0 \quad \text{for } \tau_B < \tau_c$$

where ξ = erodibility coefficient.

The model of IKEDA et al. (1981) assumes that the bank erosion rate is proportional to the near-bank primary flow velocity excess, i.e. the difference between the near-bank primary flow velocity and the mean channel velocity.

$$\frac{\partial y}{\partial t} = \xi u' \cos \theta$$

where ξ is a positive coefficient of bank erosion. This condition implies that left bank side erodes where near bank velocities are above the reach-averaged value, $u' > 0$, with consequent deposition on the adjacent right bank, and vice versa if $u' < 0$.

The model of Parker's et al. (1983) is similar to Ikeda's et al. (1981) model, the bank erosion rate increases in proportion to the velocity excess, the bank erosion equation is expressed in cartesian coordinates:

$$\frac{\partial y}{\partial t} = E_o [1 + e(u_o - 1)] u' \left[1 + \left(\frac{\partial y}{\partial x} \right)^2 \right]^{1/2}$$

where E_o and e = primary and secondary coefficients of bank erosion; the term $(u_o - 1)$ represents the reduction in reach-averaged velocity with increasing sinuosity.

BLONDEAUX & SEMINARA (1985) assume that for a small perturbation of the channel axis, the rate of bank erosion, $\partial n / \partial t$, is a function of the longitudinal shear stress, τ_b , near the bank. They followed a procedure similar to that developed by IKEDA et al. (1981):

$$\frac{\partial n}{\partial t} = E (\delta \tau_b)$$

where $\delta \tau$ is the perturbation of τ_b due to secondary flow. They implicitly assume that the unperturbed channel configuration is in equilibrium.

ROHRER'S (1983) model suggests that if the actual sediment transport at the bank is less than the transport capacity of the flow, local scour may occur and steepen the bank until it fails, leading to bank retreat.

BECK (1988) tried to improve the river meander model of IKEDA et al. (1981) by using the model of ROHRER (1983). He uses the downstream sediment transport relation and a force balance relation on a sediment particle, together with the previously determined flow and bed topography, to calculate the downstream and cross-stream sediment transport. The bank erosion rate is assumed to be proportional to the unsteady bed scour rate at the bank.

According to MOSSELMAN (1992) the some of the basic mechanisms of bank erosion are: the lateral entrainment of lower parts of the bank and near-bank bed degradation. The rate of bank retreat is proportional with the excess flow shear stress above a critical value. He concludes that input of bank erosion products makes rivers shallower and steeper. The input of bank erosion products does not affect the transverse bed slope in rivers with low banks and approximately constant width, even if those rivers are migrating fast. His model reads:

$$\frac{\partial n}{\partial t} = E_u (u_w - u_{wc}) + E_h (h_w - h_{wc})$$

where E_u and E_h account for the bank properties, u_{wc} and h_{wc} are the critical values for flow and water depth, u_w and h_w are the near-bank flow velocity and water depth respectively.

Crosato's (1990) model is based on Ikeda's et al. (1981) model, in which the flow-induced bank erosion rate is assumed simply proportional to the near-bank main velocity deformation from the reach-average value. An additional term is introduced to take into account the influence of bank height on the failure of vertical cohesive banks:

$$\frac{\partial n}{\partial t} = E_u u' + E_h h'$$

where u' : near-bank tangential velocity deformation with respect to reach-average value, h' : near-bank water depth deformation with respect to the reach-averaged value, E_u and E_h : time-averaged erosion coefficients.

3 REVIEW OF MIANDRAS MODEL

3.1 General

The quasi 2-D mathematical model **MIANDRAS** was developed by A. Crosato (1990). The model consists of two parts: the *steady flow and bed topography model* and the *bank erosion model*.

Steady flow and bed topography model

The steady flow and bed deformation model is derived from the linear version of the complete non-linear model developed by Koch & Flokstra (1980) and Struiksmas et al. (1985). The total steady deformation of the flow velocity and the water depth is determined by: deformation due to the local channel curvature and deformation due to redistribution of the flow and sediment originated from upstream changes of channel curvature. The steady deformation of the flow and channel bed is the alternate bar type. This type of deformation can be seen downstream at the entrance of a river bend: a point bar in the inner side and a pool at the outer side followed by a typical steady oscillation of the river bed, if the bend is long enough, Struiksmas et al. (1985).

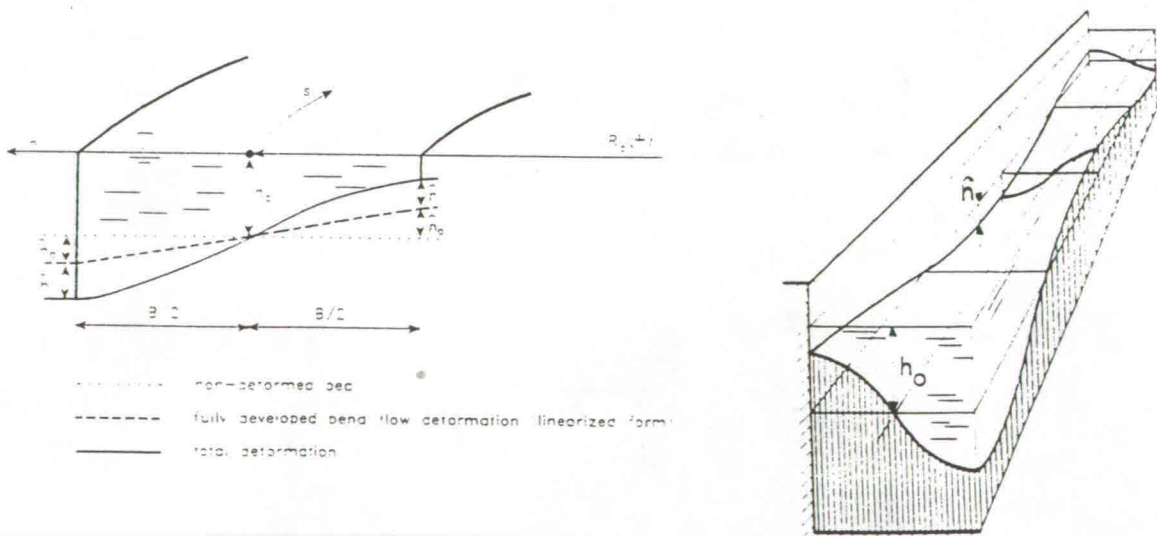


Figure 3.1.1.- Longitudinal and transversal profile of the bed, Crosato (1990).

Bank erosion model

The bank erosion model is in principle the same model as the one of Ikeda et al. (1981). The near-bank flow velocity excess from the reach-average value determines the bank erosion rate. The critical velocity for eroding banks is considered to be equal to the reach-average value flow velocity. The model includes an additional term, which accounts for the bank erosion due to bank instability.

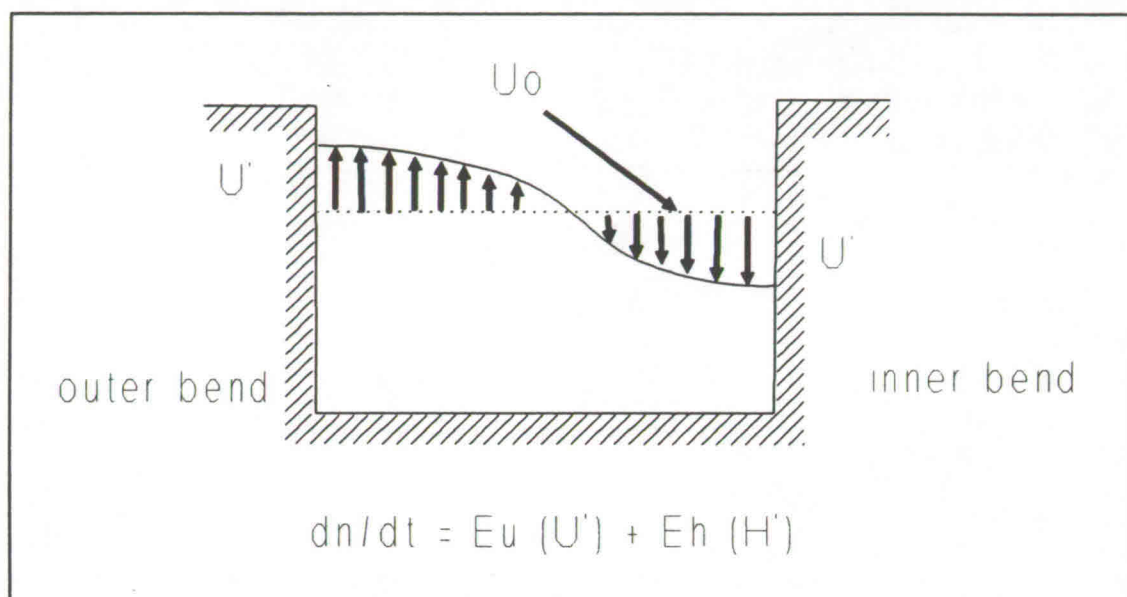


Figure 3.1.2.- Bank erosion model of MIANDRAS.

The MIANDRAS model assumptions are:

- the channel width is constant in space and time;
- the vertical pressure profile is hydrostatic;
- shallow flow approximation, h/w is small ;
- mildly curved channel approximation, w/R_c is small;
- constant hydraulic roughness (Chézy coefficient);
- the rate of sediment transport is determined by local conditions (dominant bed load);
- the influence of grain sorting is insignificant (uniform bed material);
- the Froude number is small to moderate (rigid lid approximation);
- the bed slope is mild;
- not backwater effects are accounted;
- the channel bed development is not influenced by the bank erosion products.

The description of the MIANDRAS model is presented in Appendix A.

3.2 Behaviour of the MIANDRAS model

A typical longitudinal profile of the bed along the outer bend is shown in figure 3.2.1, in which L_p is the wave length of the bed disturbance. The model behaviour can be described in terms of λ_s/λ_w , L_p and L_D , where λ_s and λ_w are the adaptation lengths for the bed and flow respectively and L_D is the damping length of the bed disturbance.

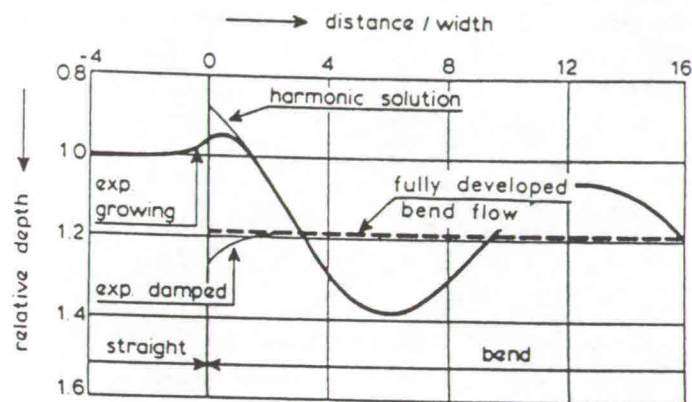


Figure 3.2.1.- Longitudinal profile of the bed along the outer bend.

The adaptation length of the flow is defined as:

$$\lambda_s = \frac{C^2 h}{2g} \quad (3.1)$$

the adaptation length of the bed topography deformation is:

$$\lambda_w = \frac{1}{(m\pi)^2} h \left(\frac{w}{h} \right)^2 f(\theta) \quad (3.2)$$

and

$$f(\theta) = \frac{0.85}{E} \sqrt{\theta} \quad (3.3)$$

where

h	water depth	[m]
w	width	[m]
C	Chézy coefficient	[-]
g	acceleration due to gravity	[m/s ²]
θ	Shields parameter	[-]
E	parameter that weighs the influence of the transversal bed slope on the bed shear stress direction	[-]
m	mode that determines the transversal pattern, being equal to 1 for meandering rivers	[-]

The value of λ_s/λ_w determines the wave length L_p of the adaptation and how quick the adaptation dampens in time via L_D , see figure 3.2.2. For low values of λ_s/λ_w correspond to gradual reduction of the height of the disturbance, therefore the system is more stable.

The expressions for the wave number and damping coefficient are:

$$\frac{2\pi}{L_p} = \frac{1}{2\lambda_w} \sqrt{(b+1) \left(\frac{\lambda_w}{\lambda_s} \right) - \left(\frac{\lambda_w}{\lambda_s} \right)^2 - \frac{(b-3)^2}{4}} \quad (3.4)$$

$$\frac{1}{L_D} = \frac{1}{2\lambda_w} \left[\frac{\lambda_w}{\lambda_s} - \frac{(b-3)}{2} \right] \quad (3.5)$$

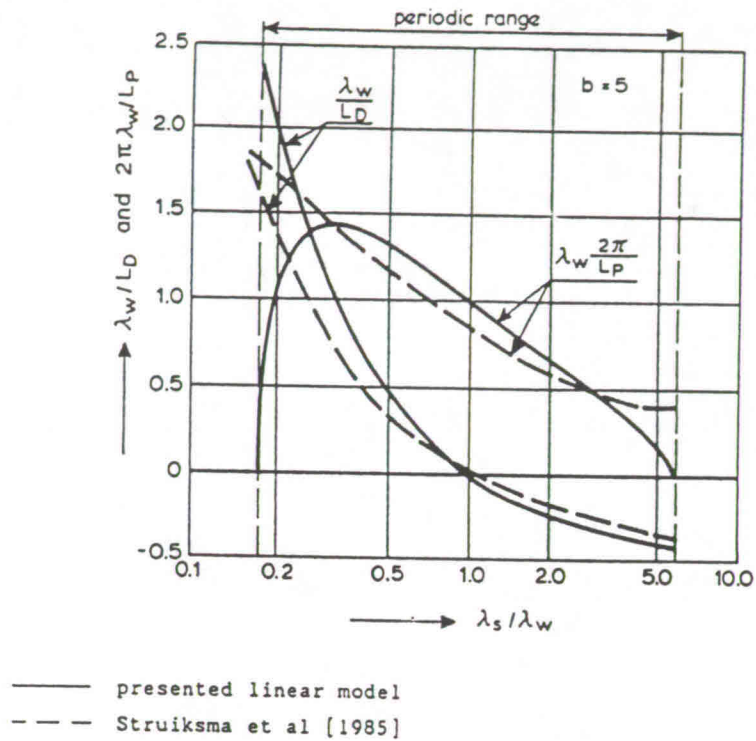


Figure 3.2.2.

The wave length L_p and the damping length L_D of the bed oscillations are highly significant for the bed development, and they are quite sensitive to the changes of the exponent b derived from the selected transport formula, see Figure 3.2.3, Struiksmas & Crosato (1989).

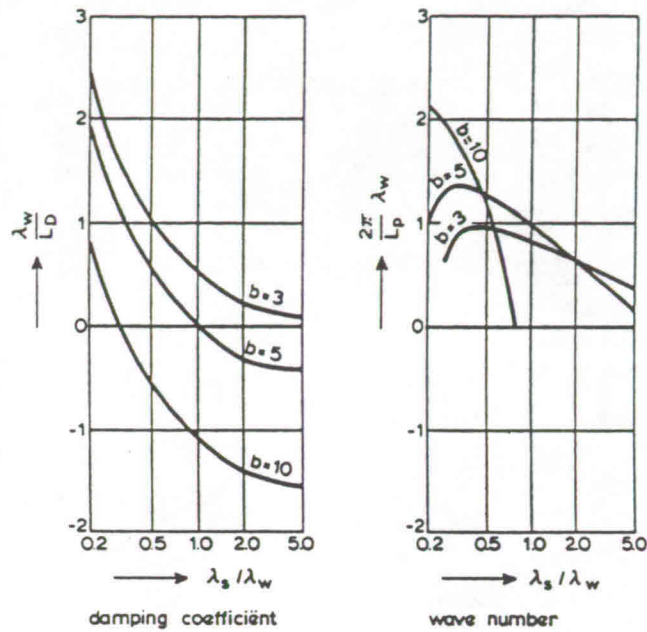


Figure 3.2.3

3.3 Modifications to the MIANDRAS model

The critical flow velocity for eroding banks is considered to be equal to the average flow velocity in the original version of MIANDRAS model. This is an incorrect assumption since the critical flow velocity that determines the bank erosion does not change in time, it has to take into account the soil properties. Therefore the correction to this model consist on taking a constant critical flow velocity, besides the bank erosion is computed at both banks. See figure 3.3.1.

The proposed bank erosion model considers that the rate of bank erosion to be proportional to the excess of near-bank flow velocity from the critical value.

For this study is not considered the bank erosion due to bank height. The original version of bank erosion model of MIANDRAS do not reproduce well this effect since bank erosion is produced with the increase of water depth due to a reduction of the bed slope. This is incorrect since higher water depths increase the stability of banks. The stability of bank reduces with the increase in water depth due to bed erosion.

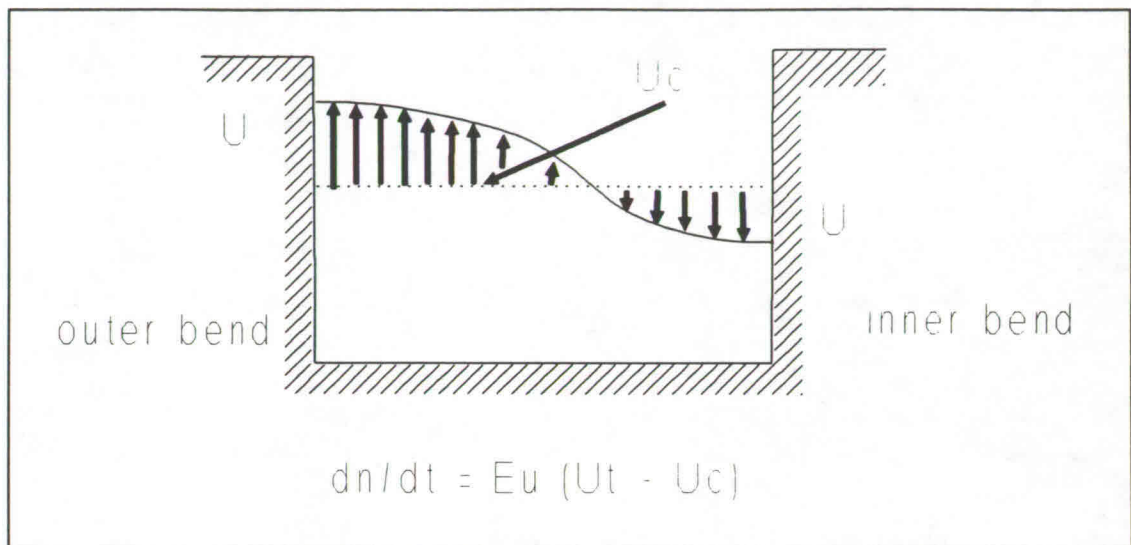


Figure 3.3.1.- Proposed bank erosion model.

4. INVESTIGATIONS

4.1 General

The erosion of river banks is the cause of lateral growth and downstream shift of river bends. High flow velocities are presented at the outer bend producing bank erosion, while low flow velocities at the inner part giving as result deposition. The river is in a constant process of adaptation along the time. See figure 4.1.1.

River bends do not grow to infinite, they reach a maximum amplitude. Some of the possible causes of river bends can reach a maximum amplitude are: *geological confinement, bend cutoffs, reduction of flow velocities due to sinuosity increases, nonlinear effects*. This study is focus only on the investigation of reaching maximum amplitude due to **reduction of flow velocities when sinuosity increases**. Chapter 1 presents a description of the causes of maximum amplitude of river bends.

One way to predict the planform development of meandering rivers is using mathematical models. The quasi 2-D MIANDRAS model, developed by Crosato (1990), is used in this study through via the improved bank erosion model.

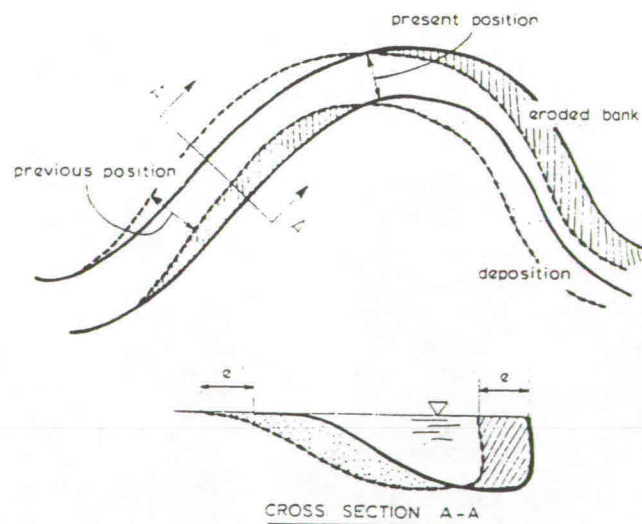


Figure 4.1.1.- Bank erosion process.

4.2 Slope reduction

The reduction of the bed slope is caused by the increase in river length when bank erosion takes place, therefore the flow velocity decreases. If the flow velocity decrease the sediment transport capacity decreases too and sedimentation occurs. When the bends are being eroded fast the longitudinal bed slope decreases simultaneously and there is not longitudinal aggradation of the bed. On the other hand, when the bank erosion is slow, aggradation of the river bed occurs. The real longitudinal bed slope can be between these two values, depending on the ratio of time-scales of both processes involved. The migration model of MIANDRAS does not account this effect.

The magnitude of the river length plays an important role in the adaptation of the longitudinal bed slope. The longer river, more time is required for the longitudinal aggradation. The aggradation wave propagates downstream.

4.2.1 Approach

Doing numerical simulations the real longitudinal bed slope can be computed, the bank erosion process can be determined as dominant or not during the adaptation process of the bed slope. The 1-D WENDY model developed by DELFT HYDRAULICS is used.

The reduction of the bed slope due to the increase in sinuosity can be simulated by the increment of the river length. This is not possible to do in the WENDY program, the river length can not be modified along the time. So, by means of extraction of sediment the reduction of the bed slope is simulated. The bank erosion and the longitudinal aggradation of the bed are simultaneously reproduced. See figure 4.2.1.1.

Figure 4.2.1.2 shows the configuration adopted for the numerical simulations, in which the upstream boundary conditions are: constant discharge and sediment transport. Constant water depth is the downstream boundary condition. The cross section is rectangular and constant along the reach. The magnitude of the extraction of sediment reduces in downstream direction.

The configuration used for the numerical simulations does not account the bank erosion effect.

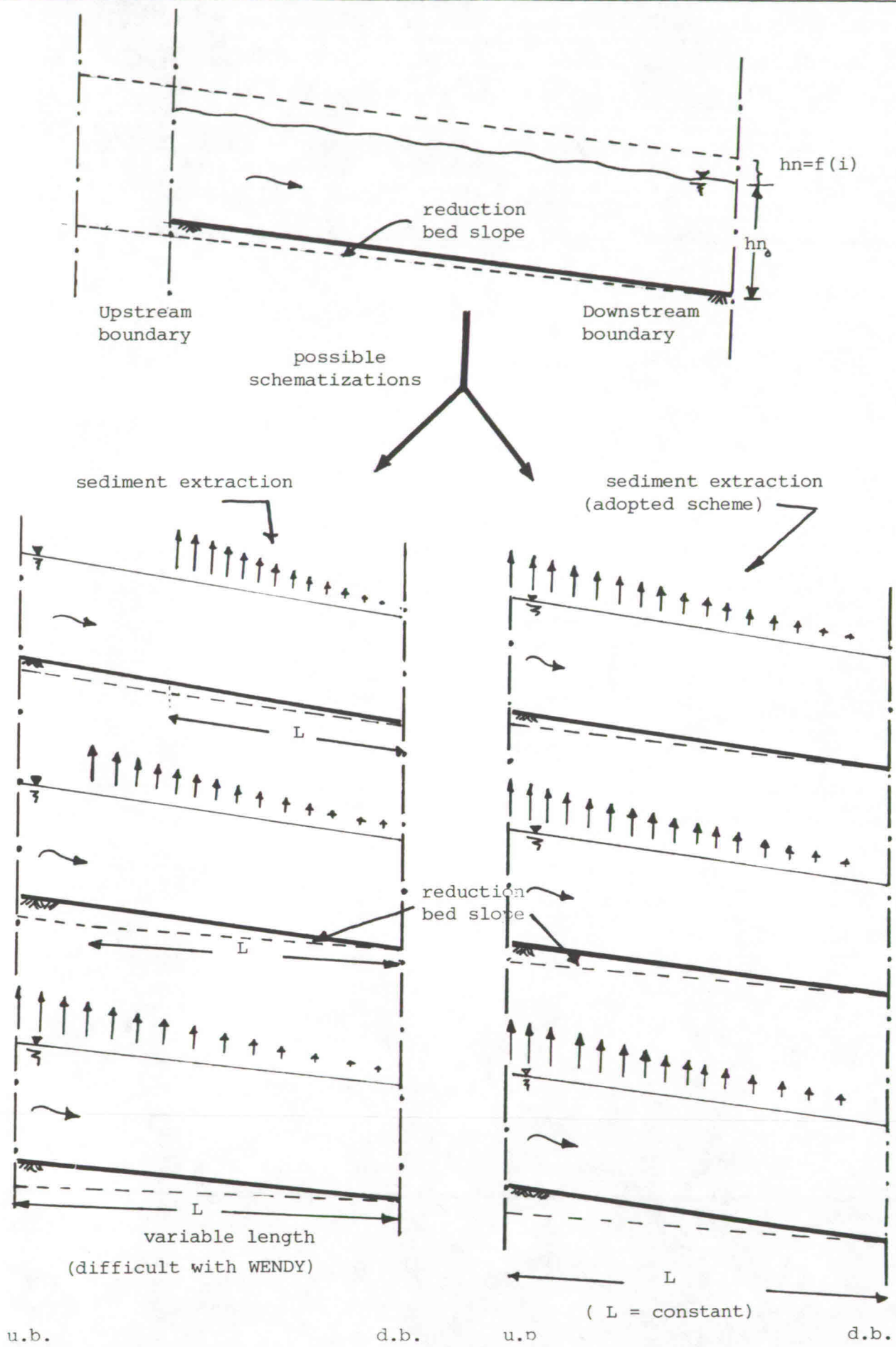


Figure 4.2.1.1.- Description of the bed slope reduction.

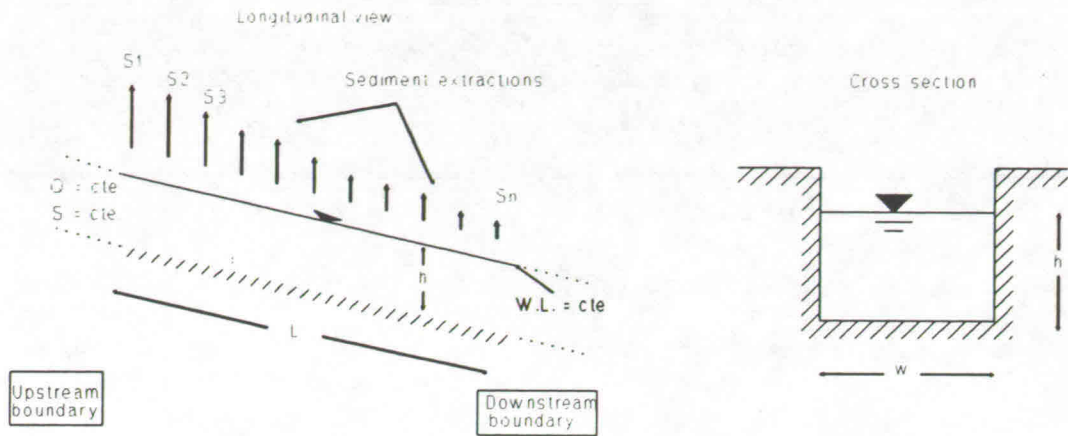


Figure 4.2.1.2.- Configuration used in the numerical simulations.

4.2.2 Time-scales

Time-scale for the bed slope due to the increase of sinuosity

The reduction of the bed slope is described in figure 4.2.2.1. The bed slope decreases faster at the initial period but later on the reduction decreases gradually. The time-scale can be approximated as:

$$T_e = \frac{i_o}{\left(\frac{di}{dt}\right)_{t=0}} \tag{4.1}$$

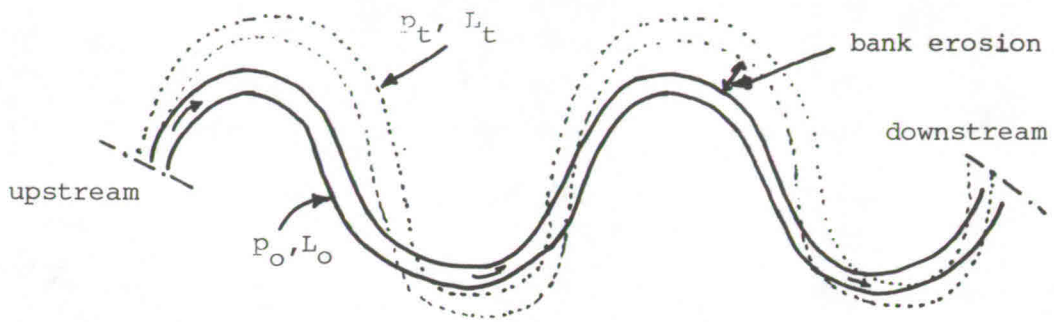
where

$$\left(\frac{di}{dt}\right)_{t=0} = -i_o \frac{C_E \xi}{L_o} \tag{4.2}$$

therefore the time scale reads:

$$T_e = \frac{L_o}{C_E \xi} \tag{4.3}$$

i_o	actual bed slope	[-]
C_E	bank erosion rate according to Hickin & Nanson (1984)	[m/s]
L_o	actual length	[m]
t	time	[s]
ξ	constant	



$p = \text{sinuosity}$

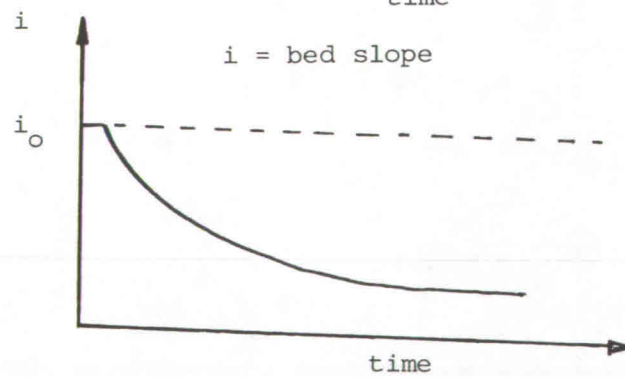
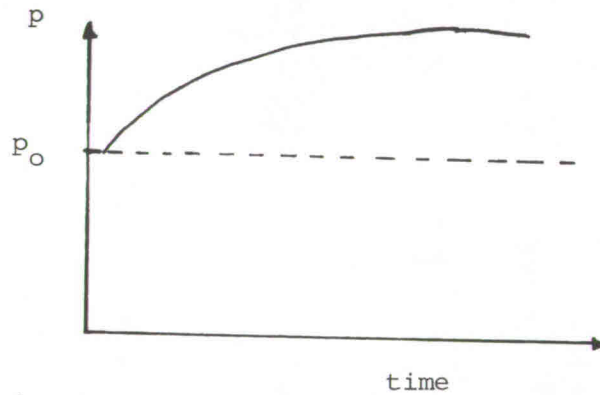


Figure 4.2.2.1- Slope reduction due to the increase of sinuosity.

Time-scale for the bed slope due to the longitudinal aggradation

The bed slope increases due to the longitudinal aggradation, this process is represented in figure 4.2.2.2. Aggradation occurs because the reduction of the sediment transport capacity of the river. The sediment propagate in downstream.

The time-scale equation presented here, is based on the study of Ribberink and Sande (1984), The mechanisms are the same. They study the aggradation in river due to overloading, the physical process is: overloading occurs in the upstream reach of the river due to external causes and due to the local transport capacity of the river is too small aggradation occurs. The aggradation wave propagates downstream.

The time-scale fo the bed slope due to the longitudinal aggradation reads:

$$T_{\text{long}} = \left[\frac{\alpha_o^2 h_o^2}{6bs_o i_o} \right] \tag{4.4}$$

where

$$\alpha = (1 - Fr^2) \tag{4.5}$$

Fr	Froude number	[-]
b	exponent of the sediment transport formula	[-]
s	sediment transport per unit width	[m ² /s]

the subscript o means actual value.

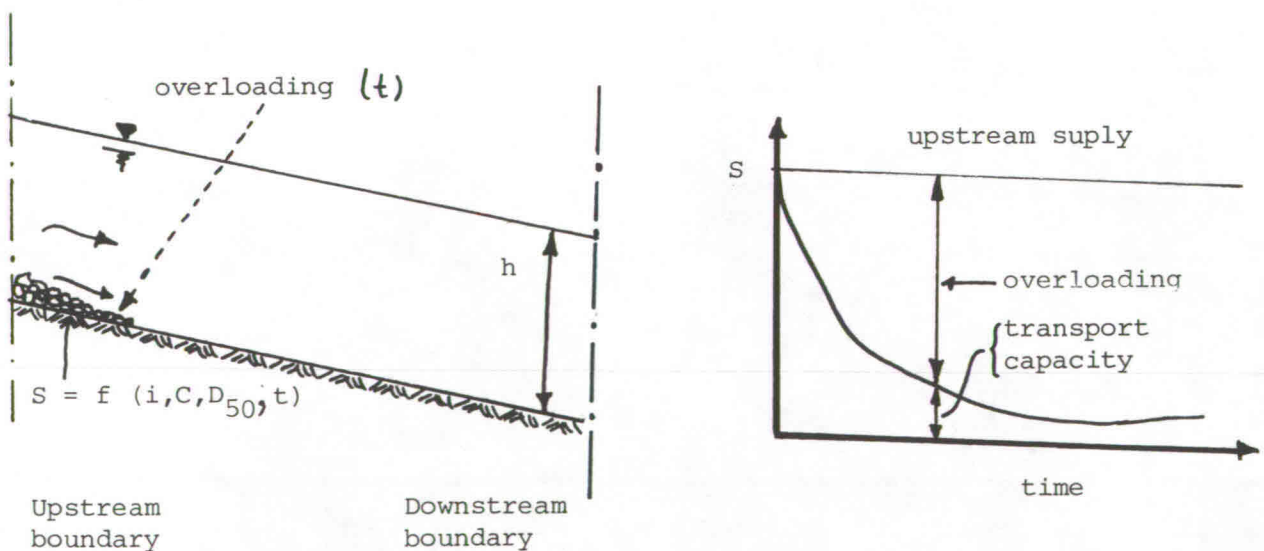


Figure 4.2.2.2- Adaptation of the bed slope due to aggradation.

4.2.3 Results

The longitudinal bed slope is determined through numerical simulations with 1-D WENDY model. With the schematization selected the simulation of the bank erosion process when sinuosity increases and the longitudinal aggradation of the bed are reproduced at the same time. The hydraulic characteristics used in the numerical simulations are based on meandering rivers data. These are:

Q =	100.0	m ³ /s
w =	50.0	m
C =	50.0	m ^{1/2} /s
i =	2.16 × 10 ⁻⁴	
D ₅₀ =	2.0 × 10 ⁻⁴	m

parameters calculated:

h =	2	m
S =	0.02	m ³ /s (computed with Engelund & Hansen formula)
c _b =	11.42 × 10 ⁻⁴	m/s
Δx =	500.0	m
Δt =	5.0	days

In the numerical simulations the Courant number is kept close to 1 for numerical stability. The Courant number is define:

$$c_b = \frac{\Delta x}{\Delta t} \quad (4.6)$$

in which

c _b	celerity of the bed disturbance	[m/s]
Δx	space-step	[m]
Δt	time-step	[m]

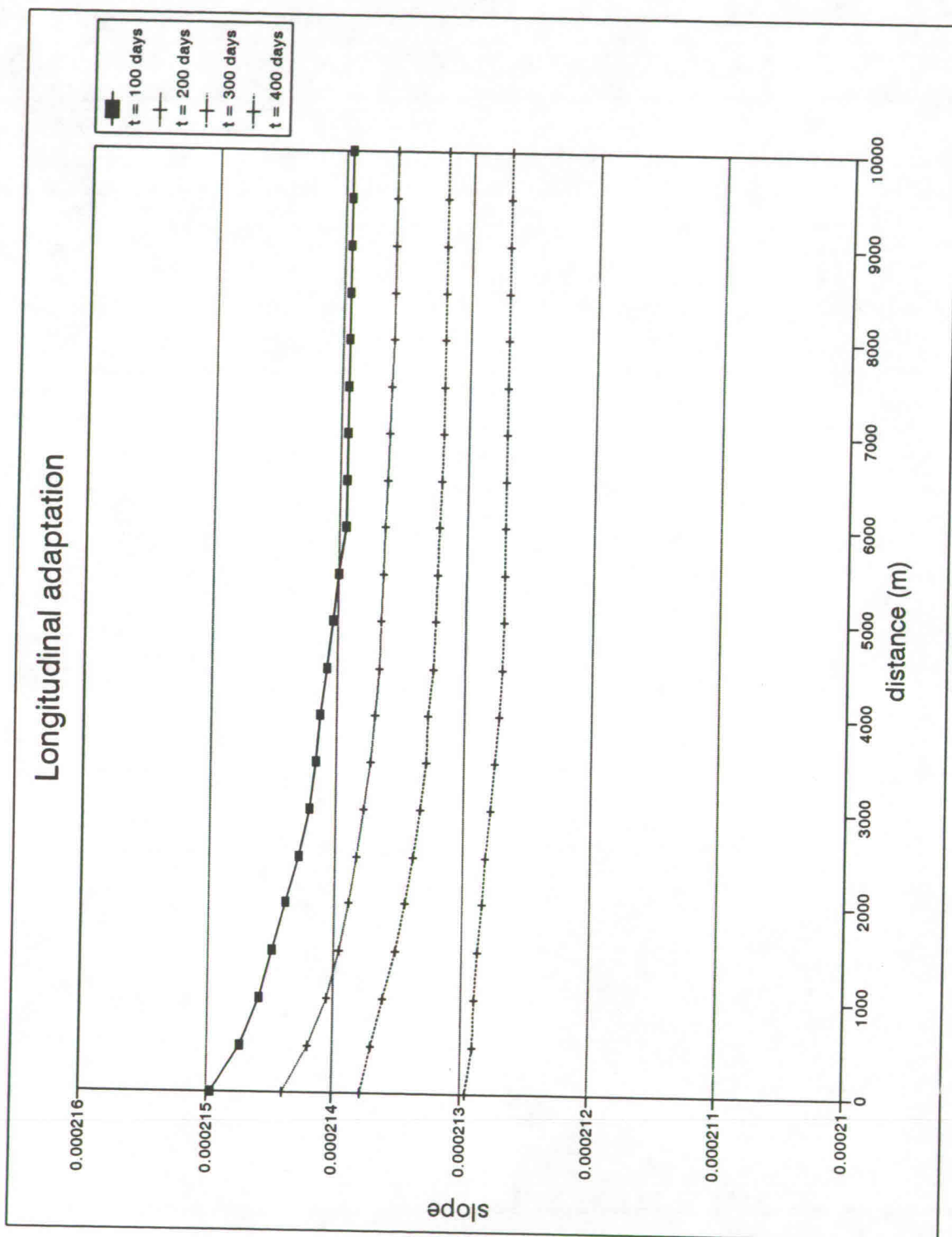
The river lengths used in the numerical simulations are: 5, 10, 20 and 25 km. These lengths were chosen according to the limitations of the study and WENDY program. The amount of sediment extraction along the reach is function of the length of the reach and the speed of the bank erosion required to be simulated. Reduction of the bed slope from 0.5 to 12% was used. Fast bank erosion corresponds to high reduction of the bed slope for a specific interval.

From the numerical simulations it can be observed the gradual adaptation of the longitudinal bed slope along the time, see figure 4.2.3.1, this figure corresponds for the case L = 10 km and with intermediate speed of the bank erosion process. From this figure it can seen that at the first stages there is difference between the upstream and downstream bed slope along the

distance and gradually this difference decreases. Afterwards the bed slope is quite constant along the river.

The value of the longitudinal bed slope for different bank erosion rates and river lengths are shown in figures 4.2.3.2, 4.2.3.3, 4.2.3.4 and 4.2.3.5. In every case the bed slope reaches an equilibrium. It can be seen from these figures, that the longer the reach the more time is required for the bed aggradation process for a specific bank erosion rate. For instance, comparing the results for $L = 5$ km and $L = 20$ km, the time required for the bed slope to reach an equilibrium for $L = 20$ km is approximately 5 times the time required for $L = 5$ km.

Figure 4.2.3.1.- Adaptation of the longitudinal bed slope for L = 10 km.



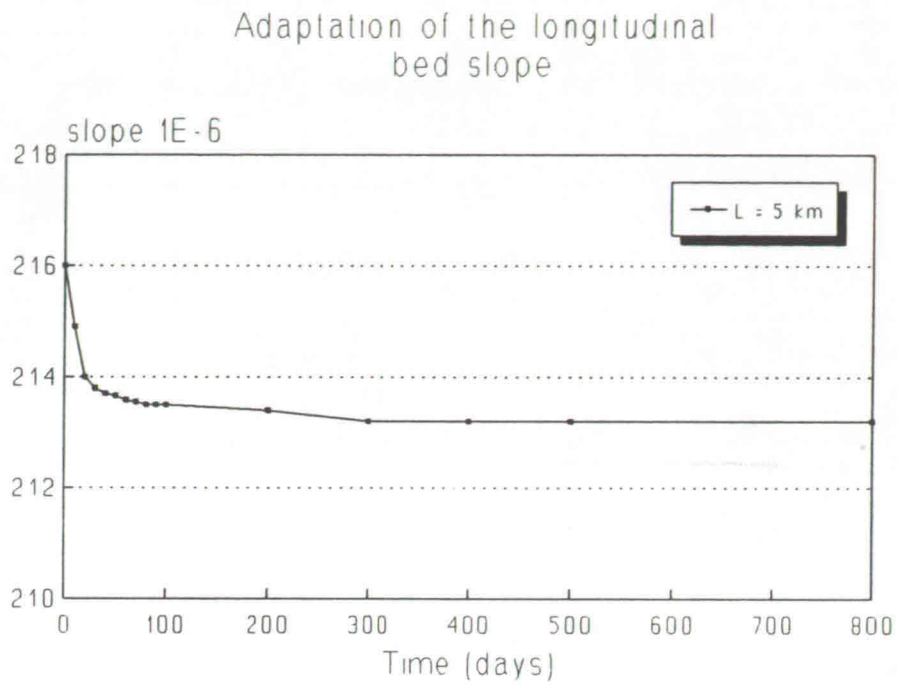
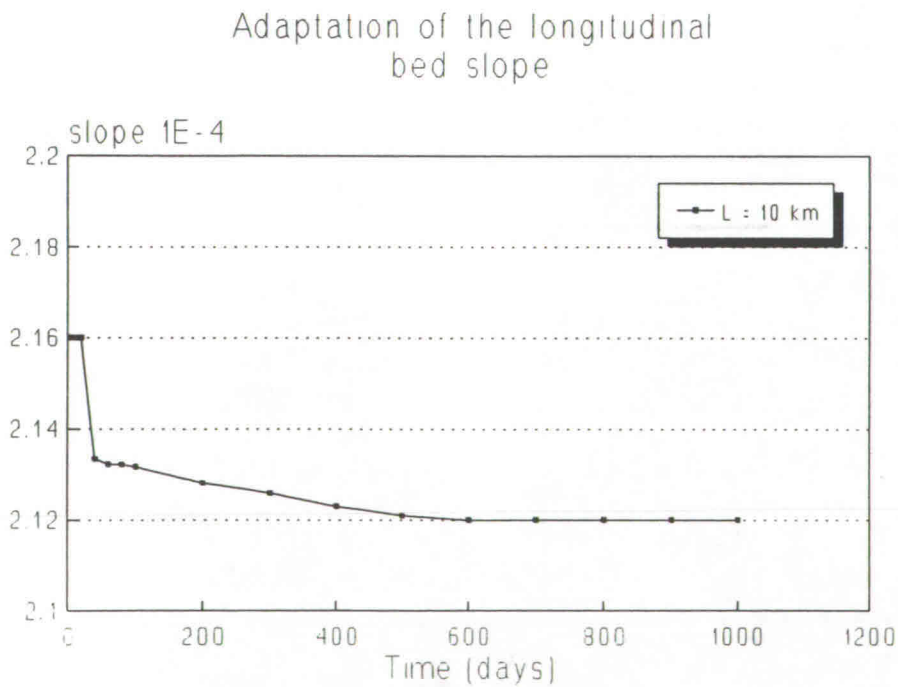


Figure 4.2.3.2



Adaptation of the longitudinal bed slope

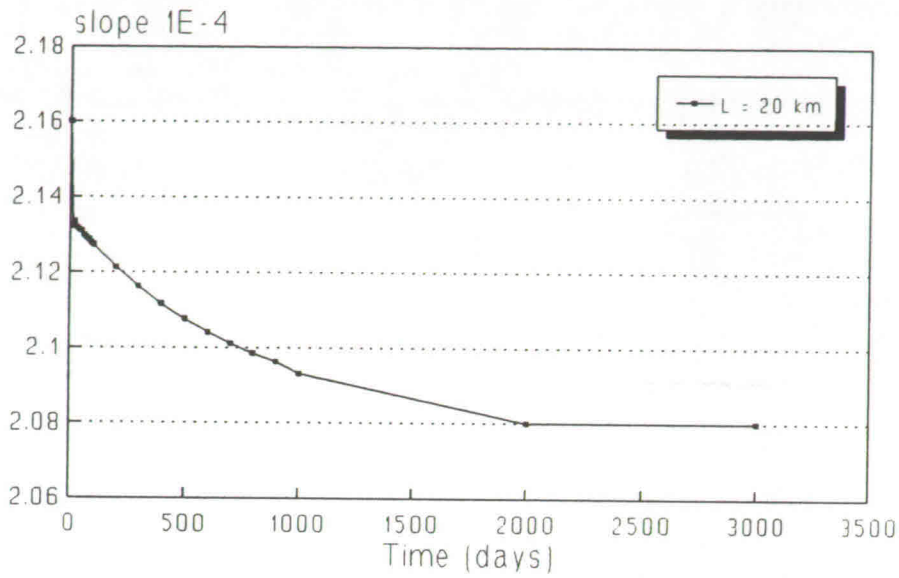


Figure 4.2.3.4

Adaptation of the longitudinal bed slope

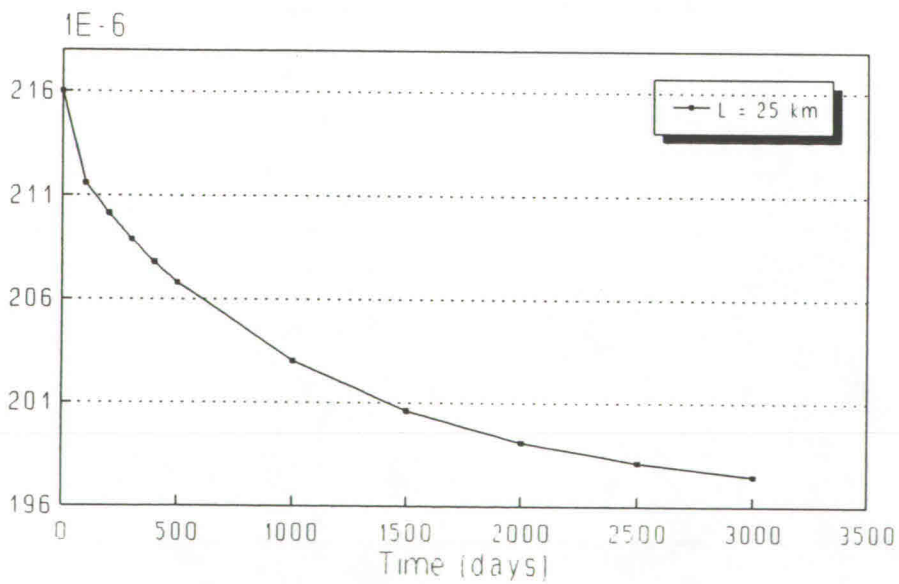


Figure 4.2.3.5

The results from the numerical simulations are useful if they are expressed in dimensionless way. The dimensionless bed slope reads:

$$i' = \frac{i_e}{i_o} \tag{4.7}$$

where

i_e bed slope in equilibrium [-]

According to Ribberink & Sande (1984) the dimensionless length is:

$$\tilde{L} = \frac{3 i}{\alpha h} L \tag{4.8}$$

The longitudinal bed slope accounting the interaction of the processes, sinuosity increases due to lateral bank erosion and bed aggradation, can be computed using the dimensionless graphs presented in figures 4.2.3.6 and 4.2.3.7.

Time scales

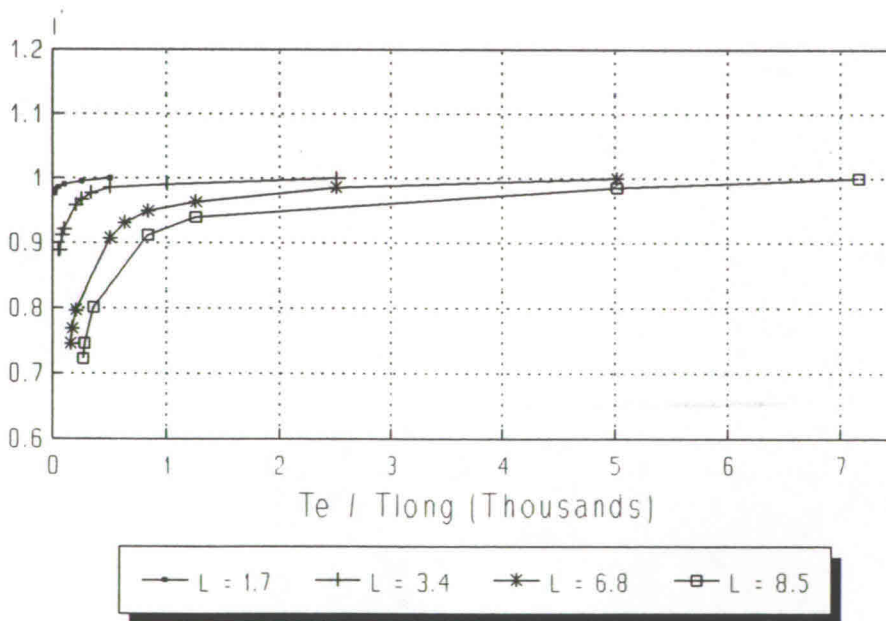


Figure 4.2.3.6

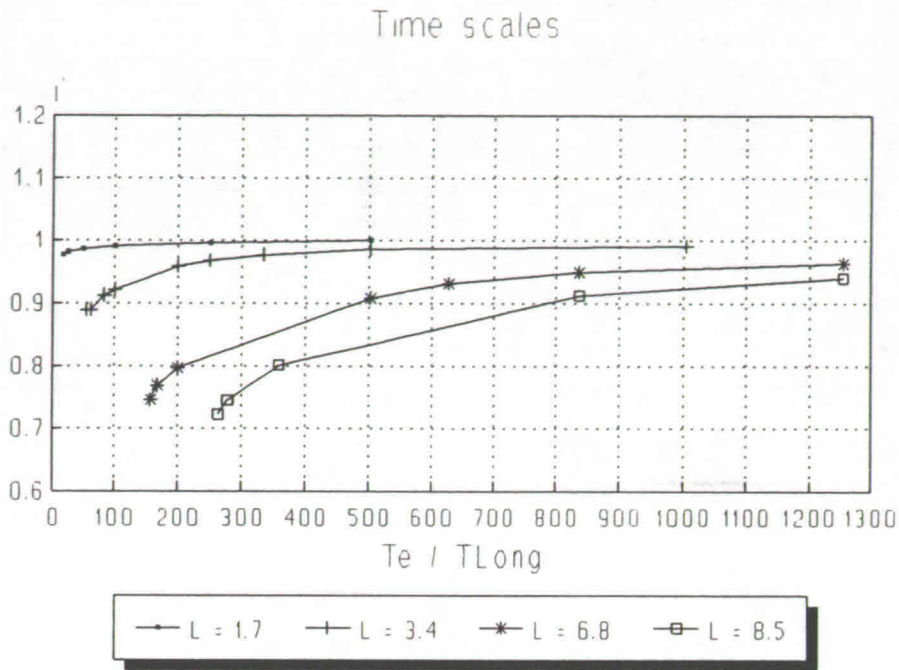


Figure 4.2.3.7

4.2.4 Importance of the bed slope reduction

The whole exercise is intended to see how important bed slope reduction can be for meandering rivers. For purpose real rivers are used, and a very rough approximation is used.

Assumptions:

- Hickin and Nanson (1984) applicable

$$r/w > 2.5$$

$$M = 0.25 M_{2.5}$$

$$Y_b = 70 \text{ N/m}^2 \text{ (opposing force per unit boundary area)}$$

- $L_o = 1/3$ total river length
- $D_{50} = 4 \times 10^{-4} \text{ m}$
- $b = 5$ (Engelund & Hansen sediment transport formula)
- $w = 8 Q^{0.5}$
- $C = 50 \text{ m}^{1/2}/\text{s}$
- $i = 2 \times 10^{-4}$

Table 4.2.4.1 shows the characteristics of some river in the world. In figure 4.2.4.1 shows their time-scales ratio computed taking the previous assumptions. The magnitude of the ratio of time-scales differs for every river. In figure 4.2.4.1 it can be seen that some rivers have high ratio of the time-scales, implying that the aggradation should be considered. For rivers with low ratio of the time-scales, the increment of the bed slope due to overloading can be neglected. Therefore, it is important to consider the ratio of time-scales in the determination of the bed slope for every river.

Table 4.2.4.1- Discharge, sediment transport and length of some rivers.

River	Q (m ³ /s)	S (m ³ /s)	L (km)
Amazon (1)	100000	19.9772	6516
Mississippi (2)	18000	6.8018	6019
Congo (3)	44000	1.7599	4700
La Plata/Parana (4)	19000	1.9026	4700
Ob (5)	12000	0.3805	5570
Nile (6)	3000	1.3794	6484
Yenissei (7)	17000	0.2473	5550
Lena (8)	16000	0.3044	4270
Amur (9)	11000	0.9989	4510
Yangtse Kiang (10)	22000	11.4155	5800
Wolga (11)	8400	0.4756	3688
Zambesi (12)	16000	2.0611	2660
St Lawrence (13)	14000	0.0824	3100
Niger (14)	5700	0.8720	4030
Murray-Darling (15)	400	0.6976	2570
Ganges (16)	14000	31.7098	2700
Indus (17)	6400	9.1324	3180
Orinoco (18)	25000	1.9581	2500
Orange river (19)	2900	3.4215	1860
Danube (20)	6400	1.5601	2850
Mekong (21)	15000	1.7757	4500
Hwang Ho (22)	4000	42.7289	4845
Brahmaputra (23)	19000	16.2354	2900
Dnjepr (24)	1600	0.0292	2285
Irrawaddi (25)	13000	6.5005	2150
Rhine (26)	2200	0.0114	1360
Magdalena (Colombia) (27)	7000	4.8833	1550
Vistula (Poland) (28)	1000	0.0301	1095
Oder (Germany/Poland) (29)	530	0.0035	912
Po (Italy) (30)	1500	0.3330	676

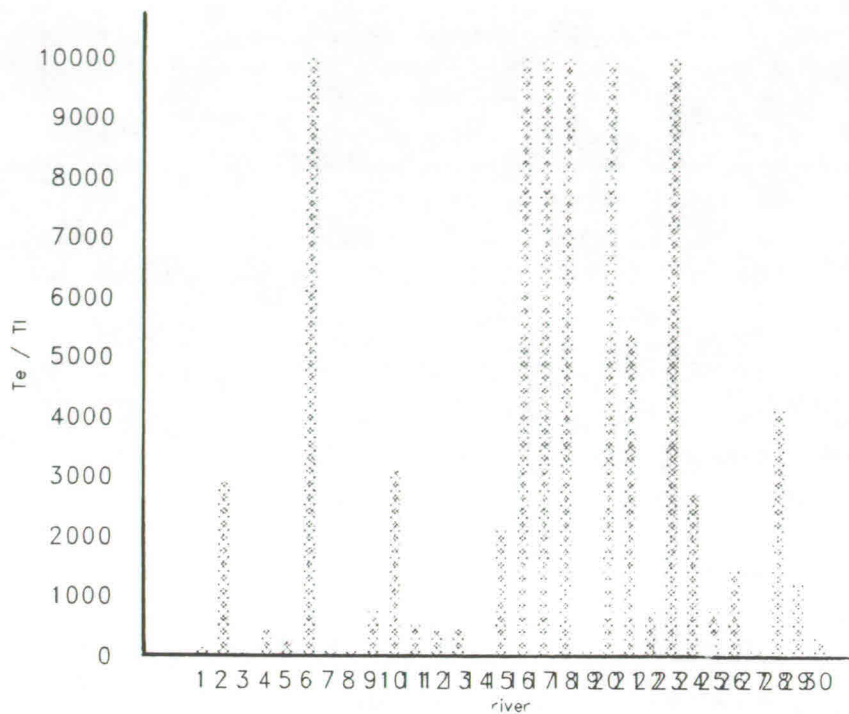


Figure 4.2.4.1.- Time-scales ratio for different rivers.

4.2.5 Conclusions

- From the comparison of the figures 4.2.3.2, 4.2.3.3, 4.2.3.4 and 4.2.3.5 it can be seen that the length of the river is an important factor. The longer the river reach, the more time it requires for reaching bed slope equilibrium. The gradual adaptation of the river bed is shown in these figures.
- The numerical simulations do not consider the influence of bank erosion products in the sediment transport and they can be significant, depending on the total volume and their characteristics. If the amount of the eroded sediments is significant, it has to be accounted for the sediment balance, because it can affect the longitudinal bed slope adaptation process. If the bank consists of a fraction ω of cohesive material, which becomes washload after being eroded, and a fraction $(1 - \omega)$ of granular material, the sediment input from bank erosion is:

$$S_E = (1 - \omega) wh \frac{dL}{dt} \quad (4.9)$$

- The results can be taken as good approximations of the phenomena simulated. Using figure 4.2.3.6 and 4.2.6.7 the new real bed slope for river can be determined.

4.3 Effect of considering $u_c = u_o$ in the bank erosion model

The zero-order flow velocity, u_o , changes its value in the migration of the river bends due to sinuosity increase: the length of the river increases. During the migration process the river is subject to a constant process of adaptation.

The bank erosion model presented by Crosato (1990) considers the average flow velocity for an infinitely long straight channel as critical velocity. The error of considering $u_c = u_o$ affects the rate of bank erosion.

Numerical simulations were carried out in order to evaluate the error of considering $u_c = u_o$. Hypothetical river planimetries are used for this purpose. Figure 4.3.1 shows the development of river bends, it is clear that the bends always grow in time because the near-bank velocities are higher than the reach-averaged velocity. River bends grow to infinity unless a cutoff is produced.

The planform development obtained using the proposed bank erosion model is presented in figure 4.3.2, $u_c \neq u_o$ (see next section 4.4). Considering $u_c \neq u_o$, the planform development is more irregular than for the case with $u_c = u_o$. The planform developments are completely different.

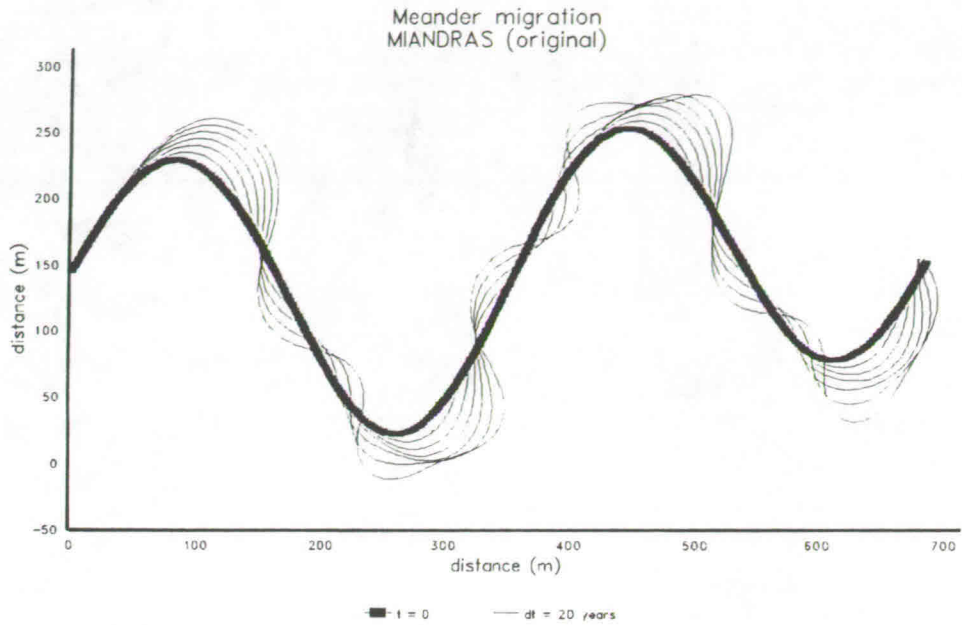


Figure 4.3.1.- Model results considering $u_c = u_0$.

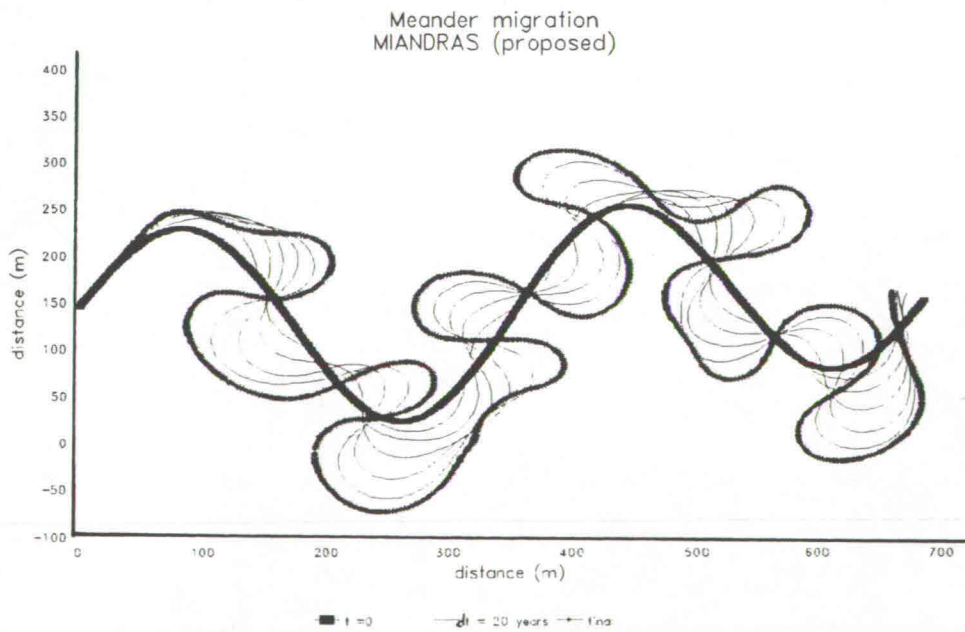


Figure 4.3.2.- Model results considering $u_c < > u_0$.

4.4. Proposed bank erosion model, $u_c \neq u_0$

The critical flow velocity that determines the rate of bank erosion has to account for the soil properties. Since the soil properties do not change in time the critical velocity for eroding bank has to be constant. The correction of the bank erosion equation consists of: the rate of bank erosion is proportional to the excess of near-banks flow velocity to a critical values. The proposed bank erosion model is:

$$\frac{\partial n}{\partial t} = E_u(u_{\text{total}} - u_c) \quad \text{for } u_{\text{total}} \geq u_c$$

$$\frac{\partial n}{\partial t} = 0 \quad \text{for } u_{\text{total}} < u_c$$

in which u_{total} is the total near-bank flow velocity at left and right bank. The second term of original model (see equation 3.1): bank erosion due to banks height is not consider in the present proposed model, because it has an unreal behaviour. For instance, when the water depth increases due to the reduction of the bed slope bank erosion occurs, this is completely illogic since an increase of water depth the stability of bank increases too and no erosion is expected. The only possibility of bank erosion due to the increase of bank height is when the water depth increase due to bed erosion, so the bank stability reduces and erosion occurs.

The above bank erosion equation was introduced in the MIANDRAS program developed by Crosato (1990) and the remaining simulations were done with this adopted model.

4.5 Numerical simulations

The geometry of the meanders, the characteristics of the bank and bed material and the hydraulic parameters affect the planform development of the bends. The important characteristics of meanders are: radius of curvature (r), width (w), wave length (λ), amplitude (a). The characteristics of bank and bed material play an important role for the sediment transport and bank erosion process. The hydraulic parameters are: discharge (Q), river slope (i), velocity (u) and roughness (C). These parameters determine the wave length (L_p) and damping length (L_D) of the bed oscillations.

For the simplicity of the study a set of hypothetical geometries is used. It is not possible to study every combination of geometries with different hydraulic characteristics, it is more important to understand the process behaviour involved for specific cases.

The procedure for the investigation consists of: first, sensitivity analysis of the parameters and secondly the determination of the critical velocity.

4.5.1 Sensitivity analysis of parameters

In order to determine the influence of the different model parameters a hypothetical river planimetry is used, see figure 4.5.1.1. The minimum possible magnitude of the critical flow velocity for eroding banks is used for the numerical simulations, because high rates of bank erosion can be expected and the sensitivity analysis of the parameters can be done. In the figures $u_c = 0$ is written, which implies minimum magnitude of the critical flow velocity is used. The criteria for selecting flow parameters is based on the empirical relations of different researches, Leopold & Wolman (1960), Inglis (1949), Zeller (1967) etc., a review of the empirical formulas is presented in Chapter 1.

The geometry of the hypothetical planimetry was generated with the function: $y = a \sin(2\pi/\lambda x)$, x and y cartesian coordinates, in which: $\lambda = 300$ m $a = 9$ m. Table 4.5.1.1 shows the hydraulic characteristics used for the simulations and the initial value of λ_x , λ_w , $\tau = \lambda_x/\lambda_w$, $1/L_D$ and L_p .

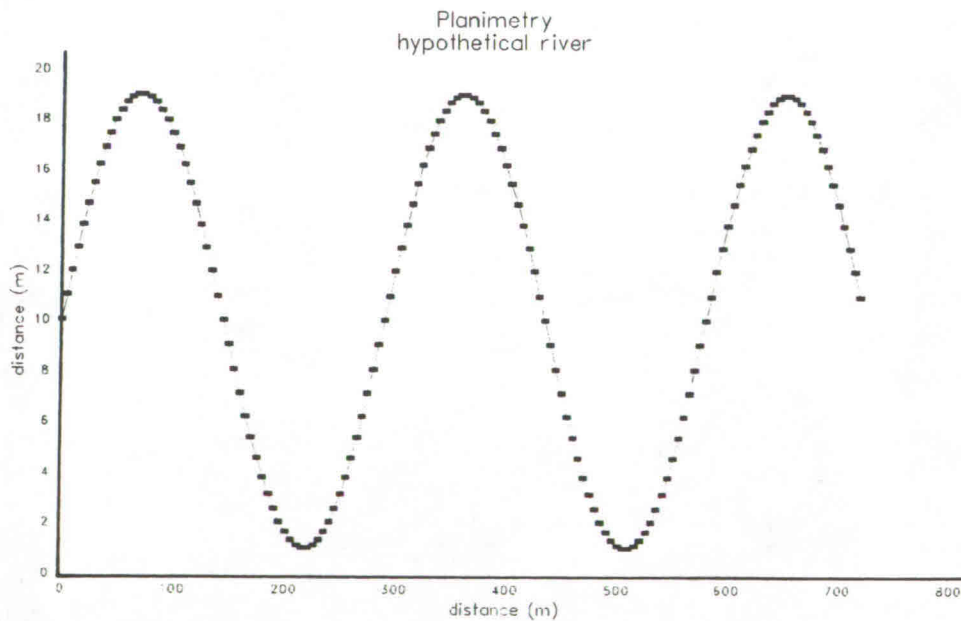


Figure 4.5.1.1.

Q [m ³ /s]	w [m]	C [m/s]	D50 [m]	lambda-s	lambda-w	r1	1/Ld [1/m]	Lp [m]
10	18	50	0.00075	18.71	71.41	0.26	0.024	480.93
10	18	50	0.00055	21.85	71.41	0.31	0.021	450.04
10	18	60	0.00075	16.61	44.38	0.35	0.023	219.89
10	18	60	0.00055	23.22	91.06	0.26	0.020	829.62
10	20	50	0.00075	23.92	66.56	0.36	0.018	358.30
10	20	50	0.00055	27.94	66.57	0.42	0.016	373.78
8	20	50	0.00075	25.77	57.36	0.45	0.015	299.82
8	18	50	0.00075	20.15	61.54	0.33	0.021	332.78
8	18	50	0.00055	23.53	61.54	0.38	0.013	275.98
8	20	50	0.00055	30.09	57.36	0.53	0.014	322.66
6,8,10,8,6	18	50	0.00055					

Table 4.5.1.1.

Influence of the discharge

Floods inevitably occur periodically in natural alluvial rivers; their magnitude and duration may affect considerably the planform development of the meanders. Two cases are analyzed: constant and variable discharge.

The magnitude of the discharge determines the water depth and the flow velocities for a specific width, channel roughness. Higher values of discharge will produce high rates of bank erosion. Figure 4.5.1.2 corresponds to a constant discharge whereas figure 4.5.1.3 is for the case of variable discharge.

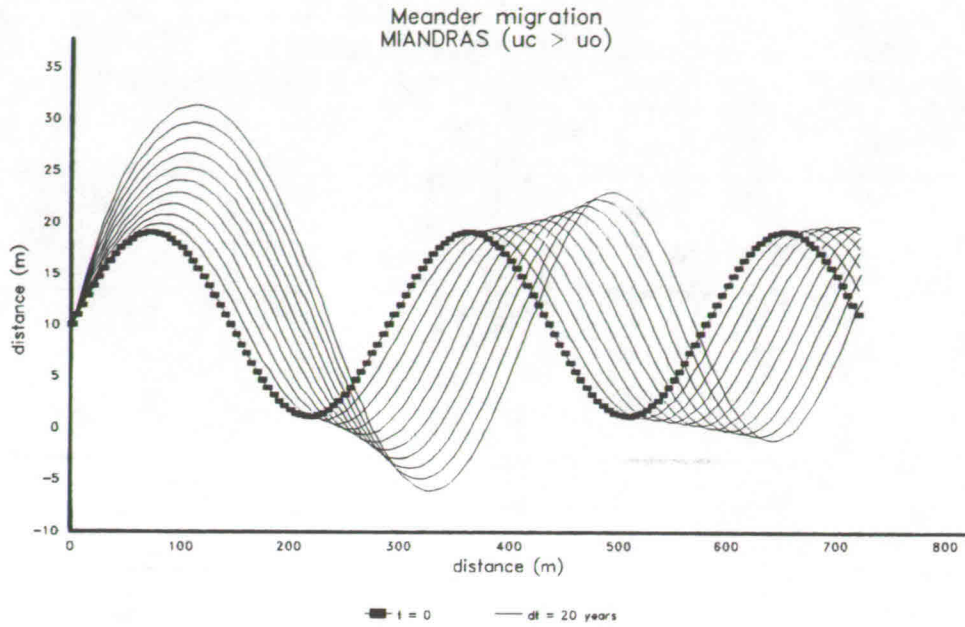


Figure 4.5.1.2.- Planform development of bends with constant discharge.

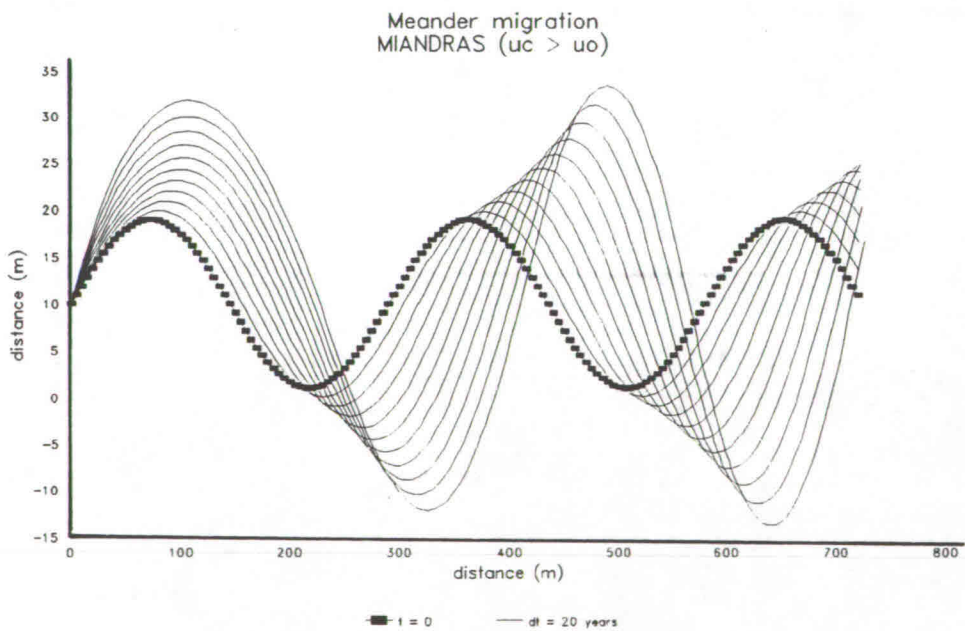


Figure 4.5.1.3.- Planform development of bends with variable discharge.

Influence of the river width

A reduction of the river width will decrease the value of the interaction parameter, λ_s/λ_w , and the river bed will become more stable because the damping length decreases, therefore less bank erosion is expected. From figure 4.5.1.4 it is verified that a smaller channel width leads to stabilization of the river bends.

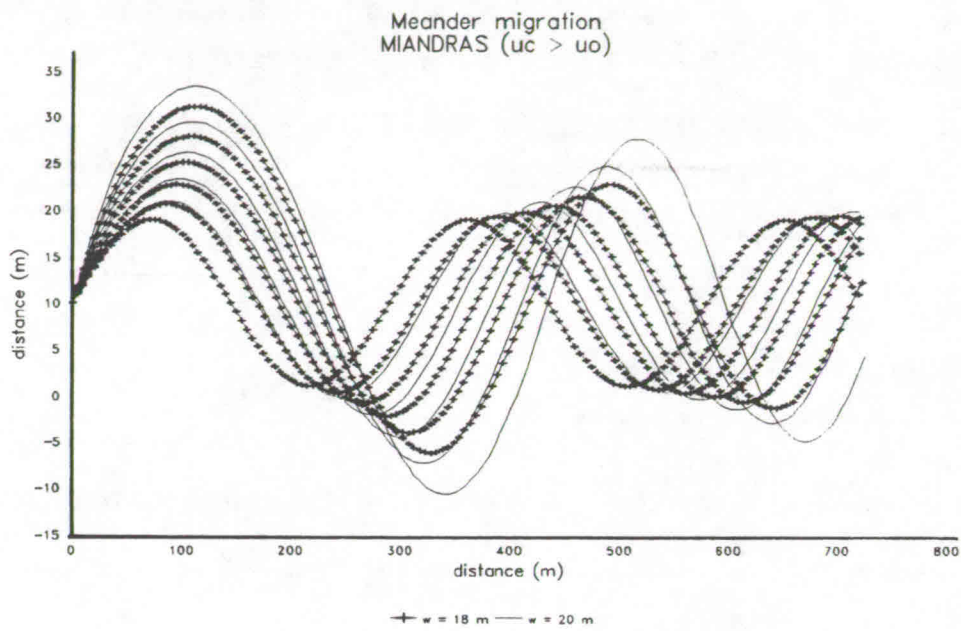


Figure 4.5.1.4.- Planform development of bends with different channel widths.

Influence of the bed roughness

Higher values of the bed roughness increase the magnitude of the adaptation length of the bed deformation, λ_w , producing a reduction of the height of the deformation because the damping increases, see figure 4.5.1.5.

$$\lambda_w = \frac{C^2 h}{2g}$$

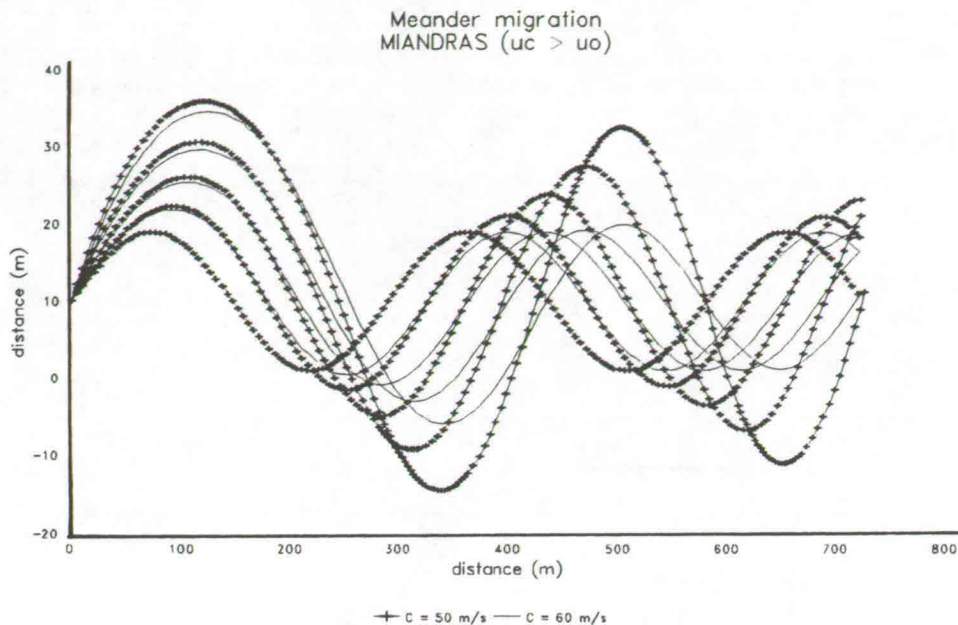


Figure 4.5.1.5.- Planform development of river with different roughness.

Influence of the bed material

The size of the bed material affects the sediment transport, higher flow velocities are required to transport big bed particles. A reduction of the diameter of the particles of the bed will increase the sediment transport, the Shields parameter increases, therefore the adaptation length of the bed, λ_s , increases too. With an increase of the adaptation length of the bed the interaction parameter increases and the system is more unstable and more bank erosion is expected. A comparison of the bends development with different size of bed material is presented in figure 4.5.1.6.

Influence of the sediment transport formula

The bed development is highly influenced by the magnitude of the wave length, L_p , and the damping length, L_D . These lengths are sensitive to the exponent b of the sediment transport formula used, $S = m u^b$. According to the Engelund & Hansen formula (total load transport) b is constant and equal to 5. However, according to Meyer-Peter & Müller formula (bed load transport), b is a function of the Shields parameter and can be relatively large and strongly variable when the Shields parameters is close to its critical value (incipient motion). Figure 4.5.1.7 shows the effect on the planform development if the Engelund & Hansen or Meyer-Peter & Müller is selected. For the study of maximum amplitude of meanders the Engelund & Hansen formula is selected, it reads:

$$s = \frac{0.08}{(s-1)^2 g^{1/2} D_{50} C^3} u^5$$

s : sediment transport per unit width [m²/s]

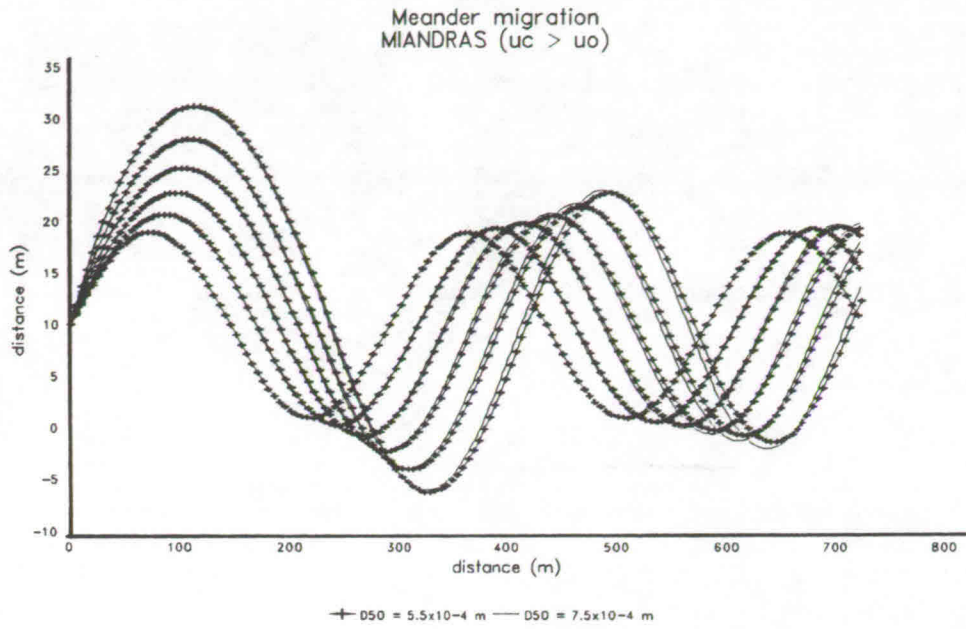


Figure 4.5.1.6.- Planform development of bends considering different bed material.

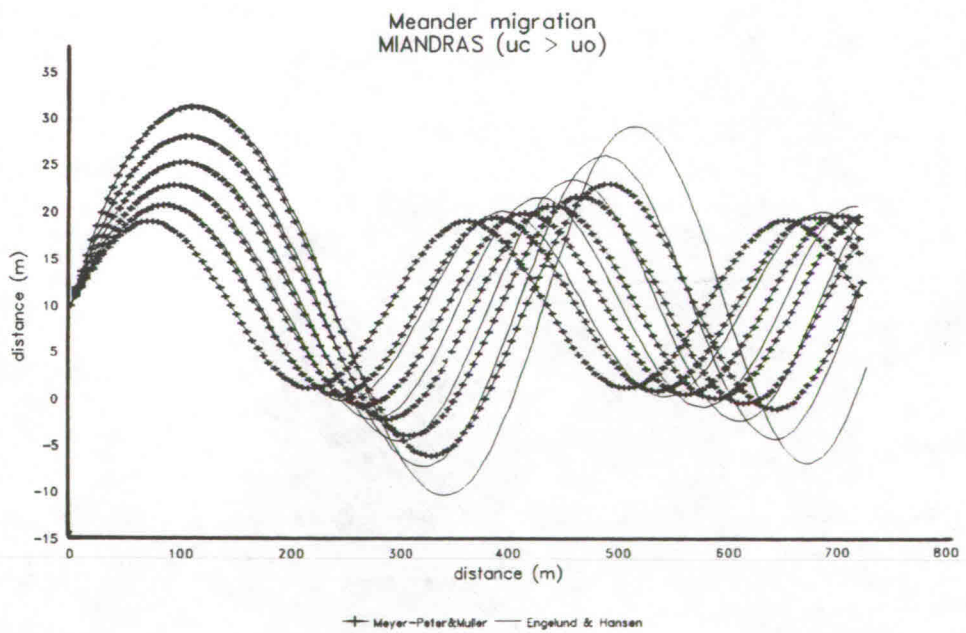


Figure 4.5.1.7.- Influence of the exponent b (sediment transport formula).

4.5.2 Critical flow velocities and maximum amplitude of river bends

The lateral expansion and translation of meander bends can be analyzed from the comparison of the values of wave length and damping length of the bed disturbance in relation to the bend length. An example is presented in figure 4.5.2.1, in which the length of the bend is different from the lengths of the bed deformation. It is concluded that longer lengths of the bed deformation will produce translation and lower values causes expansion of the bends. This is important because longer lengths of the bed deformation will produce lower near-bank flow velocity and therefore less bank erosion rate. This observation can be used for the study of bends with finite amplitude.

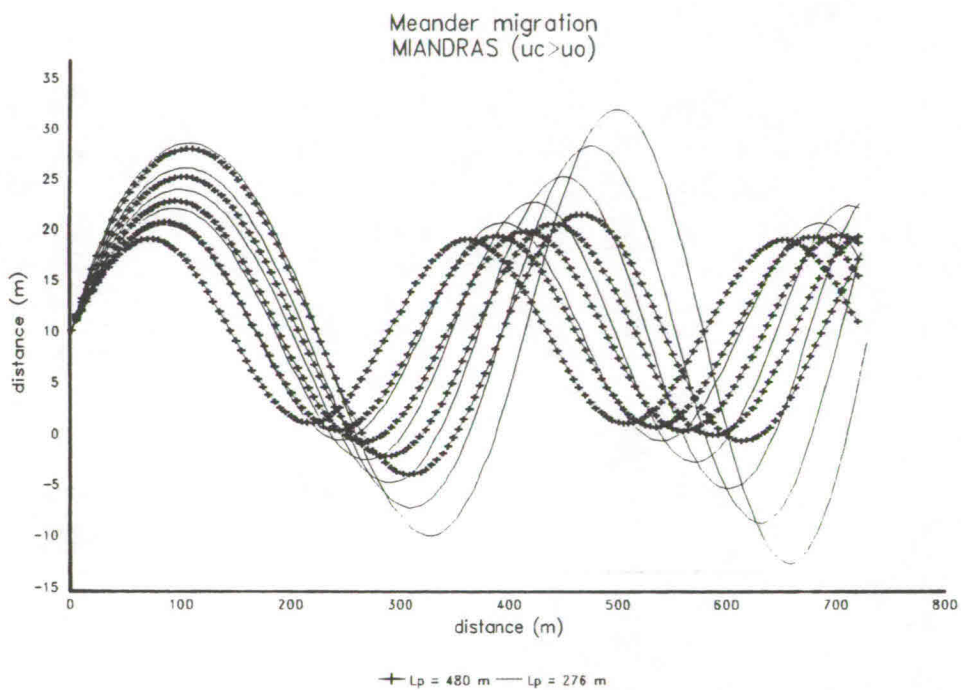


Figure 4.5.2.1.- Planform development.

With the analysis of the flow profile of the river it is possible to make an estimation of the order of magnitude of the critical flow velocity required to stop the expansion of the bends. In figure 4.5.2.2 is shown the flow profile for the hypothetical planimetry at $t = 0$. The geometry and hydraulic parameters used in the numerical simulations are described in section 4.5.1. From the figure 4.5.2.2 can be seen that the maximum flow velocities locus downstream of the bend apex. In order to compare the influence on the magnitude of critical flow velocity for eroding banks, two cases are presented in figures 4.6.2.3 and 4.6.2.4, $u_c = 0.96$ m/s and $u_c = 1.02$ m/s respectively. The value of the critical flow velocity has to be higher than 1.02 m/s to stop the expansion of the bends, otherwise the bends can not reach a finite amplitude.

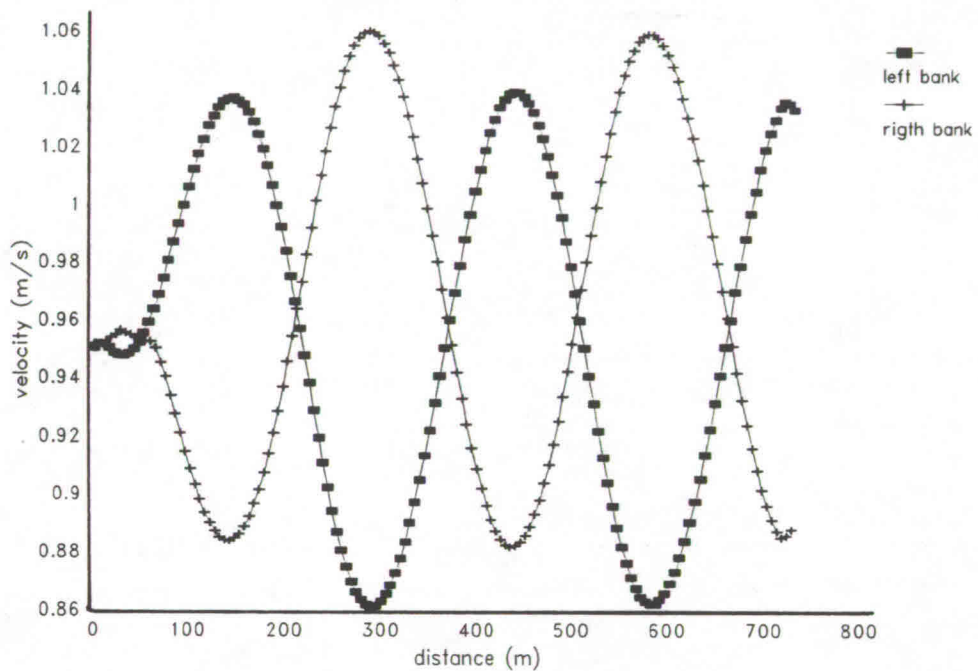


Figure 4.5.2.2.- Flow profile at both banks.

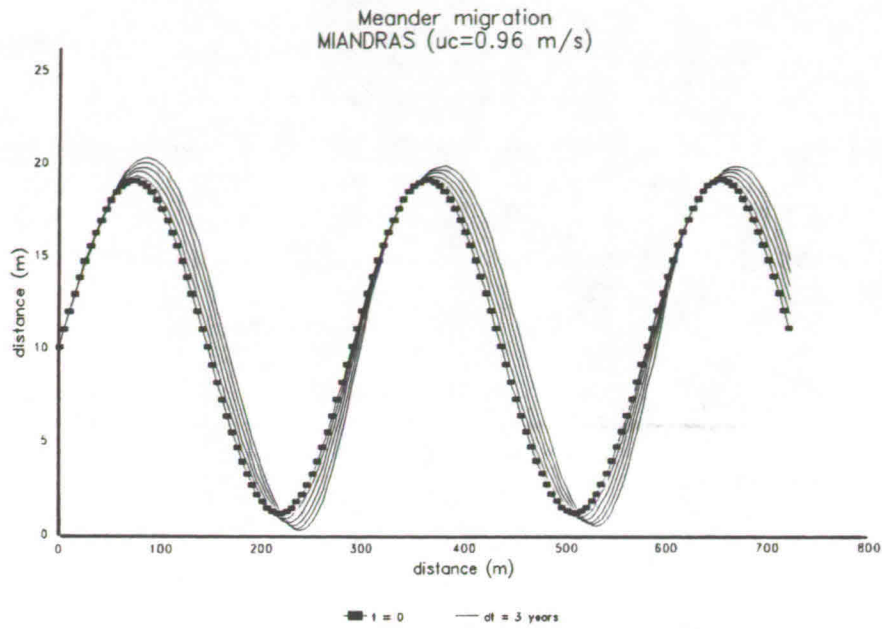


Figure 4.5.2.3.- Planform development.

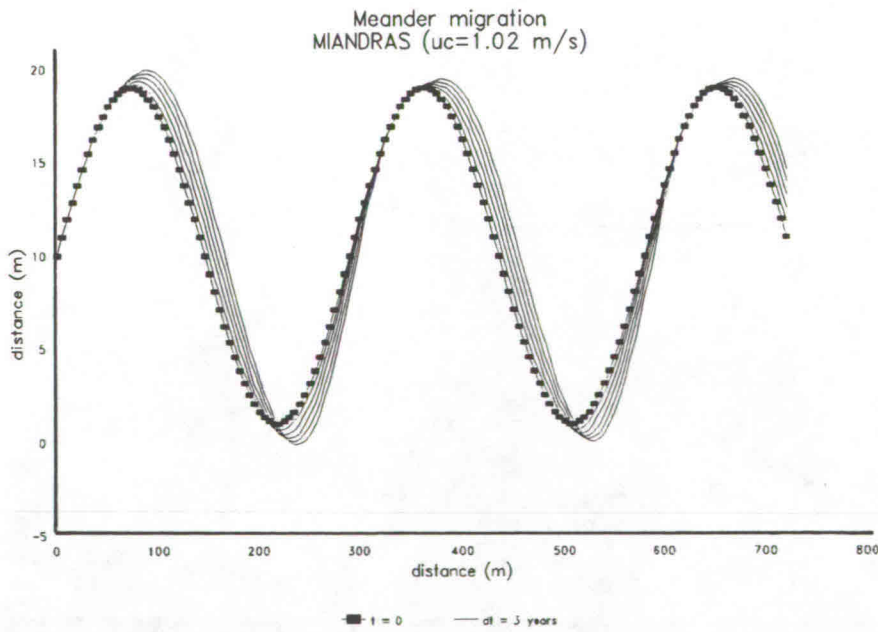


Figure 4.5.2.4.- Planform development.

Now selecting the value of the critical flow velocity to be equal to 1.04 m/s less bank erosion is produced, but gradually the lateral expansion of the bends decrease till there is not expansion of the bends, only translation is observed. The explanation of the process for this case is the next: at the beginning the bends grow, there is expansion and translation of the bends, therefore the sinuosity starts to increase. With the increment in sinuosity the flow velocities decrease in magnitude. So every time the rate of bank erosion decreases too, because it is proportional to the excess near-bank flow velocity (at both banks) to the critical flow velocity. With the reduction of the bank erosion rate the sinuosity of the river remains approximately the same, but the maximum flow velocities locus downstream of the bend apex giving as result translation of the bends. Therefore the magnitude of the flow velocity influence the development of the bends. See figure 4.5.2.5.

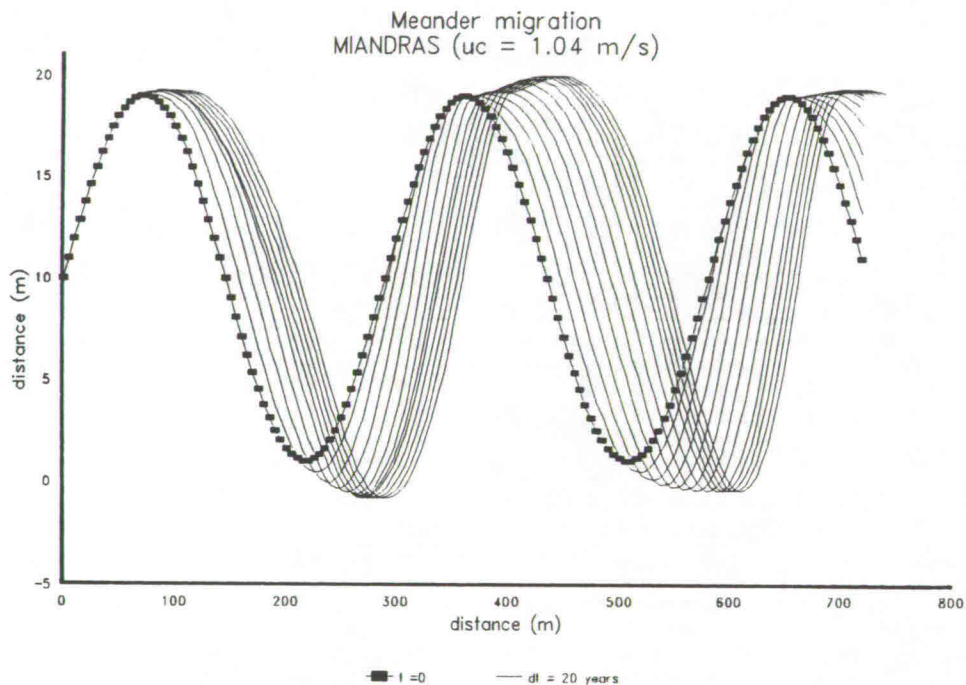


Figure 4.5.2.5.- Planform development with finite amplitude.

5. CONCLUSIONS AND RECOMMENDATIONS

Based on the present study the following conclusions can be drawn and recommendations can be given:

- Floods inevitably occur periodically, with a fairly behaviour. The characteristics of the floods change in time producing high impacts on the development of meanders, both in the magnitude and the location of the bank erosion. The migration of the river is directly affected by the magnitude of the discharge.
- Prediction of the development of meanders can be done using mathematical models, like MIANDRAS model used here. The bank erosion model proposed here considers the rate of bank erosion to be proportional to the excess of the near-bank flow velocity with respect to a critical value, gives good results.
- The behaviour of the MIANDRAS model was studied in numerical simulations using hypothetical planimetries. The development of meanders is found to be influenced by several parameters. Among the most important ones:
 - the geometry of the river,
 - the value of the interaction parameter, λ_s/λ_w , via the wave length, L_p , and the damping length, L_D , of the bed deformation in bends,
 - the value of the critical flow velocity for eroding banks.

The channel width is an important factor for the planform development. If the width is reduced the L_D of the bed disturbance will be reduced and increase L_p , therefore the river bed is more stable. The bed development is highly affected by the value b of the transport formula. Translation of bends is dominant for low values of λ_s/λ_w .

- The ratio of the time-scales of the bank erosion and the adaptation of the longitudinal bed slope have to be considered in mathematical models. Until now this is not done. When the lateral bank erosion of bends is fast compared to the longitudinal aggradation the longitudinal bed slope can decrease. Depending of the length of the river the lateral bank erosion and the related bed slope reduction is important.
- The second term of the original bank erosion model of MIANDRAS (see Crosato, 1990), which accounts for the bank height is not realistic. Including this term in the bank erosion equation mentioned, erosion occurs when the water depth increases due to the reduction of the bed slope. This is not possible since a higher water depth increases the stability of the banks.
- The order of magnitude of the critical flow velocity required for a bend to reach a maximum amplitude can be estimated from the actual flow profile. This is considered as first approximation.
- Meander bends reach a finite amplitude by increasing their sinuosity through bend erosion, decreasing flow velocities yielding a gradual reduction of the bank erosion.

- The reduction of the bed slope due to the increase of the sinuosity has to be determined taking into account the ratio of the time-scales of the processes involved. In the MIANDRAS model this effect should be accounted for.
- The bank erosion model of MIANDRAS was applied here only for hypothetical cases. It is recommended apply the model also to real river planforms as can be found in nature.

APPENDIX A

MIANDRAS MODEL

The quasi 2-D mathematical model **MIANDRAS** was developed by A. Crosato (1990). The model consists of two parts: *steady flow and bed topography model* and the *bank erosion model*.

A.1 Underlying equations

Mathematical flow models for rivers with curved alignment can be described most conveniently in a curvilinear co-ordinate system, in which the *s*-axis coincides with the channel axis, the *n*-axis is horizontal and perpendicular to the *s*-axis and the *z*-axis is vertical and positive upwards. The figure A.1 shows the curvilinear system used in the models.

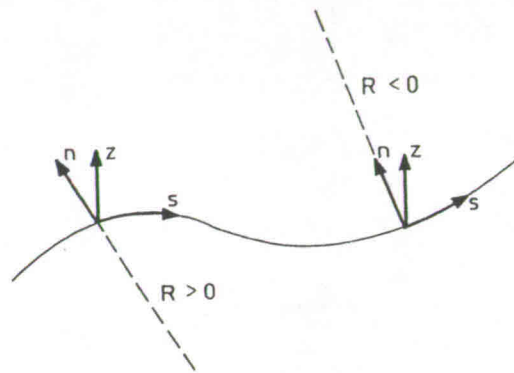


Figure A.1.- The curvilinear co-ordinate system.

Momentum and continuity equations for the flow

$$u \frac{\partial u}{\partial s} + v \frac{\partial u}{\partial n} + \frac{uv}{(R_c + n)} + g \frac{\partial z_w}{\partial s} + \frac{gu\sqrt{u^2 + v^2}}{C^2 h} = 0 \quad (\text{A.1})$$

$$u \frac{\partial v}{\partial s} + v \frac{\partial v}{\partial n} - \frac{u^2}{(R_c + n)} + g \frac{\partial z_w}{\partial n} + \frac{gv\sqrt{u^2 + v^2}}{C^2 h} = 0 \quad (\text{A.2})$$

$$\frac{\partial(hu)}{\partial s} + \frac{\partial(hv)}{\partial n} + \frac{hv}{(R_c + n)} = 0 \quad (\text{A.3})$$

where:

<i>u</i>	depth-averaged longitudinal flow velocity	[m/s]
<i>v</i>	depth-averaged transverse flow velocity	[m/s]
<i>h</i>	water depth	[m]
R_c	radius of curvature of the channel centreline	[m]

z_w	water level	[m]
C	Chezy coefficient	[m ^{1/2} /s]
g	acceleration due to gravity	[m/s ²]

in which the equations A.1 and A.2 are the longitudinal and transverse momentum equations respectively, while equation A.3 is the continuity equation.

Continuity equation for the sediment

$$\frac{\partial z_b}{\partial t} + \frac{\partial s_s}{\partial s} + \frac{\partial s_n}{\partial n} + \frac{s_n}{(R_c + n)} = 0 \quad (\text{A.4})$$

where:

z_b	bed level	[m]
s_s	volumetric component of the sediment transport in s direction per unit of width	[m ² /s]
s_n	volumetric component of the sediment transport in n direction per unit of width	[m ² /s]

Sediment transport

$$S = \omega m u^b \quad (\text{A.5})$$

The sediment transport can be computed with Engelund & Hansen, Meyer Peter & Müller or any other relation.

Direction of the bed shear stress

The effect of the spiral motion on the direction of the bed shear stress, δ , is included (Koch & Flokstra, 1980):

$$\delta = \arctan\left[\frac{v}{u}\right] - \arctan\left[A \frac{h}{R_*}\right] \quad (\text{A.6})$$

where:

$$A = \frac{2\alpha}{\kappa^2} \left[1 - \frac{\sqrt{g}}{\kappa C} \right] \quad (\text{A.7})$$

A	coefficient that weighs the influence of the spiral motion, the velocity profile is considered logarithmic, Jansen (1979);	[-]
R_*	effective local radius of curvature of the stream-line	[m]
κ	Von Karman constant	[-]
α	calibration coefficient	[-]

Direction of the sediment transport

The direction of the sediment transport, α , does not coincide with the direction of the bed shear stress, δ , due to the gravity force acting on the grains moving along a sloping bed:

$$\tan \alpha = \frac{\sin \delta - \frac{1}{f(\theta)} \frac{\partial z_b}{\partial n}}{\cos \delta} \quad (\text{A.8})$$

where:

$$f(\theta) = \frac{0.85}{E} \sqrt{\theta} \quad (\text{A.9})$$

$$\theta = \frac{u^2 + v^2}{C^2 \Delta D_{50}} \quad (\text{A.10})$$

$f(\theta)$	weighing function for the influence of the sloping bed according to Odgaard (1981)	[-]
E	calibration parameter that weighs the influence of the transverse bed slope	[m]
θ	Shields parameter	[-]
Δ	relative submerged density of the sediment	[-]
D_{50}	median particle size of bed material	[m]

if the direction of the bed shear stress is replaced in the previous equation and δ is assumed to be small, it reads:

$$\tan \alpha = \frac{v}{u} - \frac{Ah}{R_s} - \frac{1}{f(\theta)} \frac{\partial z_b}{\partial n} \quad (\text{A.11})$$

Stream-line curvature

It is approximated according to de Vriend's (1981) equation:

$$\frac{1}{R_s} = \frac{1}{(R_c + n)} - \frac{1}{u} \frac{\partial v}{\partial s} \quad (\text{A.12})$$

ZERO-ORDER EQUATIONS

These are the continuity and Chézy equations, which describe uniform flow in an infinitely long straight channel:

$$\frac{Q}{w} = u_o h_o \quad (\text{A.13})$$

$$u_o = C \sqrt{h_o i_o} \quad (\text{A.14})$$

in which:

Q	discharge	[m ³ /s]
w	width	[m]
C	Chézy coefficient	[m ^{1/2} /s]
h _o	average water depth	[m]
u _o	average flow velocity	[m/s]
i _o	longitudinal bed slope	[-]

A.2 Steady-state flow and bed deformation model

The general equations are combined in order to define the flow and bed deformation model, the equations are simplified via linearization, which means that every quantity can be divide in two terms, the reach-averaged value (infinitely long straight channel) and a perturbation term:

$$\begin{aligned} u &= u_o + U' && \text{for } U' \ll u_o \\ h &= h_o + H' && \text{for } H' \ll h_o \\ S_b &= S_o + S'_b && \text{for } S'_b \ll S_o, \text{ etc.} \end{aligned}$$

Flow deformation

$$\begin{aligned} \frac{\partial}{\partial s} \left(\frac{\partial U'}{\partial n} \right) + \frac{1}{\lambda_w} \frac{\partial U'}{\partial n} - \frac{u_o}{2\lambda_w h_o} \frac{\partial H'}{\partial n} + u_o \frac{\partial}{\partial s} \left(\frac{1}{R_c} - \frac{1}{u_o} \frac{\partial V'}{\partial s} \right) + \\ + \frac{u_o}{2\lambda_w} \left(\frac{1}{R_c} - \frac{1}{u_o} \frac{\partial V'}{\partial s} \right) = 0 \end{aligned} \quad (\text{A.15})$$

Bed deformation

$$\frac{\partial H'}{\partial s} - \frac{h_o}{f(\theta_o)} \frac{\partial^2 H'}{\partial n^2} - (b-1) \frac{h_o}{u_o} \frac{\partial U'}{\partial s} + A h_o^2 \frac{\partial}{\partial n} \left(\frac{1}{R_c} - \frac{1}{u_o} \frac{\partial V'}{\partial s} \right) = 0 \quad (\text{A.16})$$

in which the adaptation length of the tangential flow velocity (λ_w) is define: $\lambda_w = C^2 h / 2g$. For details of the derivation and linearization of the equations see Crosato (1990).

The total deformation of flow velocity (U') and water depth (H') are determined by: deformation due to the local channel curvature (u'_o, h'_o) plus the deformation caused by the redistributions of flow and sediment (u', h'). The perturbations of the flow velocity and water depth are:

$$\begin{aligned} U' &= u'_o + u' \\ H' &= h'_o + h' \end{aligned}$$

u'_o, u', h'_o, h' are determined by:

$$\frac{\partial h'_o}{\partial n} = \frac{Af(\theta)h_o}{R_c} \quad (\text{A.17})$$

$$\frac{\partial u'_o}{\partial n} = \frac{u_o}{2h_o} \frac{\partial h'_o}{\partial n} - \frac{u_o}{2R_c} \quad (\text{A.18})$$

$$h' = \hat{h} \sin(k_B n) \quad (\text{A.19})$$

$$u' = \hat{u} \sin(k_B n) \quad (\text{A.20})$$

where the wave number in the transverse direction, k_B , is defined as:

$$k_B = \frac{m\pi}{w} \quad (\text{A.21})$$

Equations A.17 and A.18 correspond to the fully developed bend flow conditions.

Total solution of the equations

The solution of the flow and bed deformation equations is determined with the sum of the solution of their homogeneous parts and one solution of the equations for fully developed bend flow conditions (non-homogeneous equations), Crosato (1990). The total near-banks deformation equations are:

$$\begin{aligned} \frac{\partial U}{\partial s} + \frac{U}{\lambda_w} &= H \left[\frac{1}{2\lambda_w} \frac{u_o}{h_o} \right] - \frac{u_o}{k_B} \frac{\partial}{\partial s} \left[\hat{c} + \frac{1}{R_c} \left(\frac{m\pi}{2} \right) \right] - \\ &- \frac{(2-\sigma)}{2\lambda_w} \frac{u_o}{k_B} \left[\hat{c} + \frac{1}{R_c} \left(\frac{m\pi}{2} \right) \right] \end{aligned} \quad (\text{A.22})$$

with:

$$\frac{\partial H}{\partial s} + \frac{H}{\lambda_s} = (b-1) \frac{h_o}{u_o} \frac{\partial u}{\partial s} + A h_o k_B \left[\hat{c} + \frac{1}{R_c} \left(\frac{w}{2} \right) \right] \quad (\text{A.23})$$

$$\lambda_s = \frac{1}{(m\pi)^2} h \left(\frac{w}{h} \right)^2 f(\theta) \quad (\text{A.24})$$

$$\hat{c} = \frac{1}{u_o} \frac{\partial K}{\partial s} \left[\frac{R_c^2}{1 + R_c^2 k_B^2} \right] \left[k_B + \frac{1}{R_c} \right] \quad (\text{A.25})$$

$$K = - \left[\frac{u_o}{h_o} \frac{\partial \hat{h}}{\partial s} + \frac{\partial \hat{u}}{\partial s} \right] \quad (\text{A.26})$$

$$\begin{aligned} U &= \hat{u}_o + \hat{u} \\ H &= \hat{h}_o + \hat{h} \end{aligned}$$

where:

U	near-bank total deformation of the main velocity	[m/s]
H	near-bank total deformation of water depth	[m]
\hat{h}_o	near-bank deformation of the water depth	[m]
\hat{u}_o	near-bank deformation of the main velocity	[m/s]
σ	coefficient that weighs the effects of the secondary flow momentum convection	[-]

and the magnitudes of \hat{u}_o and \hat{h}_o are computed with:

$$\hat{h}_o = f(\theta_o) h_o A \frac{1}{R_c} \left(\frac{w}{2} \right) \quad (\text{A.27})$$

$$\hat{u}_o = \left(\frac{1}{2} \frac{u_o}{h_o} \right) \hat{h}_o - \frac{u_o}{2} \frac{1}{R_c} \left(\frac{w}{2} \right) \quad (\text{A.28})$$

A.3 Bank erosion model

Many factors influence bank erosion process in the rivers. Flow parameters may be the most important factor for the analysis and study of bank erosion. During bank erosion process the river bends grow laterally and migrate in downstream direction, the slope decreases, the flow velocity and the shear stress decrease. Due to the reduction of the flow velocities and the shear stress the river bank stability increases.

The flow-induced rate of bank erosion is assumed simply proportional to the near-bank tangential velocity excess from the reach-averaged value. Therefore, the model is the same as Ikeda et al. (1981) but with additional terms that accounts the failure of banks due to their height. The model reads:

$$\frac{\partial n}{\partial t} = E_u(u-u_o) + E_h(h-h_o) \quad (\text{A.29})$$

$$u = u_o + U$$

$$h = h_o + H$$

where

E_u	flow-induced bank erosion coefficient	[-]
E_h	bank-instability-induced bank erosion coefficient	[1/s]

The banks properties are taken in these erosion coefficients.

According to the bank erosion model the critical velocity is the reach-averaged value, so this critical velocity changes with time if sinuosity increases.

REFERENCES

- Ariathuri R. & K. Arulanandan**, "Erosion rates of cohesive soils", *J. Hydr. Div., ASCE*, vol. 104, No. HY2, pp. 279-283, 1978.
- Beck S.M.**, "Computer-simulated deformation of meandering river patterns", Ph.D. thesis, Univ. of Minnesota, U.S.A, 1988.
- Brice J.C.**, "Planform properties of meandering rivers", in: *River Meandering, Proc. Rivers 1983*, New Orleans, Ed. C.M. Elliott, ASCE, pp. 1-15, 1984.
- Blondeaux P. & G. Seminara**, "A unified bar bend theory of river meanders", *J. Fluid Mech.*, vol. 157, pp. 449-470, 1985.
- Crosato, A.**, "Simulation of meandering river processes", *Communications on Hydr. and Geotech. Engrg.*, No. 90-3, Delft Univ. of Technol., ISSN 0169-6548, 1990.
- Dury G.H.**, "Theoretical Implications of underfit streams", U.S. Geol. Survey Prof. paper 452-C, 1965.
- Engelund F.**, "Flow and bed topography in channel bends", *J. of the Hydr. Div., ASCE*, 100, pp. 1631-1648, 1974.
- Hickin E.J.**, "The development of meanders in natural river channels", *American Journal of Science*, 274, pp. 414-442, 1974.
- Hickin E.J. & G.C. Nanson**, "The character of channel migration of the Beatton river, Northeast Columbia, Canada", *Geol. Soc. of America Bull.*, 86, pp. 487-494, 1975.
- Hickin E.J. & G.C. Nanson**, "Lateral migration rates of river bends", *J. Hydr. Engrg., ASCE*, vol. 110, No. 11, pp. 1557-1567, 1984.
- Ikeda S., G. Parker & K. Sawai**, "Bend theory of river meanders, Part 1, Linear development", *J. Fluid Mech.*, vol. 112, pp. 363-377, 1981.
- Ikeda H.**, "Sedimentary controls on channel migration and origin of points bars in sand-bedded meandering rivers", in: *River Meandering, AGU, Water Resources Monograph 12*, Eds. S. Ikeda & G. Parker, pp. 51-68, 1989.
- Inglis C.C.**, "The behaviour and control of rivers and canals", *Res. Publ., Poona (India)*, No. 13, 2 vols, 1949.

- Jansen P. Ph.**, "Principles of river engineering", Pitman Publ. Ltd., London, 1979.
- Joglekar D.V.**, "Manual on river behaviour", Control and Training Central Board of Irrigation and Power, publication No. 60, 1971.
- Johannesson H. & G. Parker**, "Linear theory of river meanders", in: River Meandering, AGU, Water Resources Monograph 12, Eds. S. Ikeda & G. Parker, pp. 181-213, 1989.
- Klaassen G.J. & B.H.J. van Zanten**, "On cutoffs ratios of curved channels", XXIIth IAHR Congress, Ottawa, Canada, 21-25 August, 1989.
- Koch F.G. & C. Flokstra**, "Bed level computations for curved alluvial channels", Proc. of the XIX IAHR Congress, New Delhi, India, vol. 2, 1980.
- Langbein W.B. & Leopold L.B.**, "River meanders - theory of minimum variance", U.S. Geol. Survey, Prof. paper 422-H, 1967.
- Leopold L.B. & M.G. Wolman**, "River channel pattern: braided, meandering and straight", U.S. Geol. Survey, Prof. paper 282-B, 1957.
- Leopold L.B. & M.G. Wolman**, "River meanders", Bull. Geol. Soc. of America, vol. 71, June, 1960.
- Mosselman E.**, "Mathematical modelling of morphological processes in rivers with erodible cohesive banks", Communications on Hydr. and Geotech. Engrg., No. 92-3, Delft Univ. of Technol., ISSN 0169-6548, 1992.
- Odgaard A.J.**, "Meander flow model. I: Development", J. of Hydr. Engrg., ASCE, 112, pp. 1117-1136, 1986 a.
- Odgaard A.J.**, "Meander flow model. II: Applications", J. of Hydr. Engrg., ASCE, 112, pp. 1137-1150, 1986 b.
- Olesen K.W.**, "Bed topography in shallow river bends", Communications on Hydr. and Geotech. Engrg., No. 87-1, Delft Univ. of Technol., ISSN 0169-6548, 1987.
- Parker G., K. Sawai & S. Ikeda**, "Bend theory of river meanders, Part 2, Nonlinear deformation of finite-amplitude bends", J. Fluid Mech., vol. 115, pp. 303-314, 1982.
- Parker G., P. Diplas & J. Akiyama**, "Meander bends of high amplitude", J. Hydr. Engrg., ASCE, vol. 109, No. 10, pp. 1321-1337, 1983.
- Ribberink J.S. & J.T.M. van der Sande**, "Aggradation in rivers due to overloading", Communications on Hydr. and Geotech. Engrg., No. 84-1, Delft Univ. of

Technol., 1984.

- Rohrer W.L.M.**, "Effects of flow and bank material on meander migration in alluvial rivers", in: *River Meandering, Proc. Rivers 1983*, New Orleans, Ed. C.M. Elliott, ASCE, pp. 770-782, 1983.
- Schumm S.A.**, "River adjustment to altered hydrologic regimen-Murrumbidgee river and Paleochannels, Austria", *Usgs professional paper 598*, pp. 65, 1968.
- Seminara G. & M. Tubino**, "Weakly nonlinear theory of regular meanders", *J. Fluid Mech.*, vol. 244, pp. 257-288, 1992.
- Shen H.W.**, "Migration of the Mississippi river", U.S. Army Corps of Engineers, Vickburg, Mississippi, 1988.
- Struiksma N., K.W. Olesen, C. Flokstra & H.J. de Vriend**, "Bed deformation in curved alluvial channels", *J. Hydr. Res., IAHR*, vol. 23, No.1, pp.57-79, 1985.
- Struiksma N. & A. Crosato**, "Analysis of a 2-D bed topography model for rivers", in: *River Meandering, AGU, Water Resources Monograph 12*, Eds. S. Ikeda & G. Parker, pp. 153-180.
- Zeller**, "Meandering channels in Switzerland", *Symp. on River Morphology, Bern, IASH*, 1967.

